NASA TECHNICAL MEMORANDUM

NASA TM X-2854

NASA TM X-2854

FLIGHT INVESTIGATION OF ACOUSTIC AND THRUST CHARACTERISTICS OF SEVERAL EXHAUST NOZZLES INSTALLED ON UNDERWING NACELLES ON AN F106 AIRPLANE

by Richard R. Burley, Raymond J. Karabinus, and Robert J. Freedman

Lewis Research Center
Cleveland, Ohio 44135

NATIONAL AERONAUTICS AND SPACE ADMINISTRATION • WASHINGTON, D. C. • AUGUST 1973

1. Report No.	2. Government Accession No.	3. Recipient's Catalog No.
NASA TM X-2854		

4. Title and Subtitle	5. Report Date
FLIGHT INVESTIGATION OF ACOUSTIC AND THRUST CHARACTERISTICS OF SEVERAL EXHAUST NOZZLES INSTALLED ON UNDERWING NACELLES ON AN F106 AIRPLANE	August 1973
	6. Performing Organization Code
7. Author(s) Richard R. Burley, Raymond J. Karabinus, and Robert J. Freedman	8. Performing Organization Report No. E-7319
	10. Work Unit No. 501-24
9. Performing Organization Name and Address Lewis Research Center National Aeronautics and Space Administration Cleveland, Ohio 44135	11. Contract or Grant No.
	13. Type of Report and Period Covered Technical Memorandum
12. Sponsoring Agency Name and Address National Aeronautics and Space Administration Washington, D. C. 20546	14. Sponsoring Agency Code

15. Supplementary Notes

16. Abstract

To determine flyover noise and thrust and to investigate whether flight velocity significantly affects the noise of exhaust nozzles, a series of flight tests was conducted on three different exhaust nozzles of a type suitable for supersonic transport aircraft. The tests were conducted using an F106B aircraft modified to carry two underwing nacelles, each containing a calibrated turbojet engine. A flyover altitude of 91 meters (300 ft) and a Mach number of 0.4 provided acoustic data that were repeatable to within ±1.5 PNdB. Flyover results showed that an auxiliary inlet ejector nozzle was the quietest of the nozzles tested; flight velocity appeared to reduce its noise.

17. Key Words (Suggested by Author(s))	18. Distribution Statement
Flight velocity effect; Jet noise; Nozzle thrust; Propulsion system; Plug nozzle; Auxiliary inlet ejector; Variable flap ejector	Unclassified - unlimited

19. Security Classif. (of this report)	20. Security Classif. (of this page)	21. No. of Pages	22. Price*
Unclassified	Unclassified	48	$3.00

* For sale by the National Technical Information Service, Springfield, Virginia 22151

FLIGHT INVESTIGATION OF ACOUSTIC AND THRUST CHARACTERISTICS OF SEVERAL EXHAUST NOZZLES INSTALLED ON UNDERWING NACELLES ON AN F106 AIRPLANE

by Richard R. Burley, Raymond J. Karabinus, and Robert J. Freedman

Lewis Research Center

SUMMARY

To determine flyover noise and thrust and to investigate whether flight velocity significantly affects the noise of exhaust nozzles, a series of flight tests was conducted on three different exhaust nozzles of a type suitable for supersonic transport aircraft. The tests were conducted using an F106B aircraft modified to carry two underwing nacelles each containing a calibrated J85-GE-13 afterburning turbojet engine. Data were taken at engine power settings of military and maximum afterburner which correspond to relative jet velocities of 500 and 860 meters per second (1640 to 2820 ft/sec).

A flyover altitude of 91 meters (300 ft) and a Mach number of 0.4 provided acoustic data that were repeatable to within ±1.5 perceived noise decibels (PNdB). Flyover results showed an auxiliary inlet ejector nozzle to be the quietest and a conical plug nozzle the noisiest; the difference was about $4\frac{1}{2}$ PNdB. Also, the auxiliary inlet ejector nozzle had the highest nozzle gross thrust coefficient, 0.98. Flight velocity appeared to reduce the noise of the auxiliary inlet ejector nozzle.

INTRODUCTION

The dominant noise source during takeoff of supersonic transport aircraft is the high velocity jet issuing from the exhaust nozzle. Investigations of the acoustic characteristics of exhaust nozzles generally have been done at static conditions. In reference 1, the noise produced by an auxiliary inlet ejector nozzle, a variable flap ejector nozzle, and a plug nozzle of a type suitable for supersonic transport aircraft has recently been evaluated in a static test facility. The results showed the plug nozzle to be the quietest for static conditions and also for an extrapolated sideline distance of 305 meters (1000 ft) to simulate a flyover at this altitude.

Although these results are applicable when the takeoff speed of the aircraft is relatively low, the takeoff speeds associated with supersonic transport aircraft are relatively high, about Mach 0.35 when maximum sideline noise is recorded. As a result of these high speeds, the external air flowing across and sometimes (as with an auxiliary inlet ejector) into the exhaust nozzle could have a significant effect on the noise produced by the nozzle since the entrainment and mixing of external flow with the high velocity jet could be altered. Also, because the aircraft is in motion relative to the observer, there will be a Doppler shift of frequency and a change in the level of the spectrum.

To gain some insight into this phenomenon, a series of flyover and static tests are being conducted on exhaust nozzles. The tests use an F106B aircraft modified to carry podded engines mounted near the aft lower surface of the wing with the exhaust nozzles extending beyond the wing trailing edge. The primary jet exhaust was provided by one of the two calibrated turbojet engines (J85-GE-13). The flyover tests were conducted at an altitude of 91 meters (300 ft) and at Mach 0.4. Acoustic measurements were taken from a ground station directly beneath the flight path. For static tests, the acoustic measurements were taken at a radial distance of 30.5 meters (100 ft) from the nozzle.

A variety of basically different nozzle concepts are being used in this flight program. Results for some of the nozzles are reported in reference 2. The present report will (1) present the acoustic and thrust performance for flyover tests conducted on the same nozzle types as those in reference 1, (2) present preliminary data on the effects of flight velocity on the acoustic characteristics of these exhaust nozzles, and (3) describe the procedures used to record and analyze the acoustic data. The nozzles tested approximated the geometry appropriate for low-speed operation of variable nozzles designed for efficient operation in the Mach 2.7 range.

SYMBOLS

A	effective area, m^2 (ft^2)
a_o	speed of sound in air, m/sec (ft/sec)
b	height of plug nozzle throat (fig. 7(a)), cm (in.)
c	mean circumference of plug nozzle throat (fig. 7(a)), cm (in.)
D	nozzle drag, kN (lbf)
d_n	nozzle maximum diameter, 63.5 cm (25 in.)
d_8	primary-nozzle-exit effective diameter, cm (in.)
d_9	ejector exit diameter, cm (in.)

F	nozzle gross thrust, kN (lbf)
L	axial distance from primary nozzle exit to secondary throat, cm (in.)
L_{d_8}	axial location of primary nozzle throat, cm (in.)
L_e	axial distance from primary nozzle exit to ejector exit, cm (in.)
OASPL	overall sound pressure level, dB (ref. 2×10^{-5} N/m^2)
P	absolute total pressure, kN/m^2 (psi)
p	absolute static pressure, kN/m^2 (psi)
PNL	perceived noise level, PNdB
R_p	sound propagation distance, cm (in.)
r	radius, cm (in.)
T	absolute total temperature, K (^oR)
V_R	relative jet velocity, m/sec (ft/sec)
W	weight flow, kg/sec (lbm/sec)
γ	primary nozzle convergence angle, deg
θ	acoustic angle (fig. 13), deg
ρ	jet density, kg/m^3 (lbm/ft^3)
$\omega\sqrt{\tau}$	corrected secondary weight flow ratio, $(W_s/W_8)\sqrt{T_s/T_8}$

Subscripts:

ip	one-dimensional isentropic expansion of primary flow
s	secondary
0	free stream
8	nozzle throat

APPARATUS AND PROCEDURE

Test Facility

Flyover tests as well as some of the static tests were conducted with an F106B aircraft modified to carry two underwing nacelles. The aircraft in flight is shown in figure 1. A schematic view of the nacelle-engine installation is shown in figure 2. The 63.5-centimeter (25.0-in.) diameter nacelles were located at approximately 32 percent semispan with the exhaust nozzles extending beyond the wing trailing edge. Because the

nozzle would interfere with normal elevon movement, a section of the elevon immediately above each nacelle was cut out and rigidly fixed to the wing. Each nacelle contained a calibrated J85-GE-13 afterburning turbojet engine. The nacelles had normal shock inlets with blunted cowl lips for the flyover tests. Secondary air to cool the engine and afterburner was supplied from the inlet and was controlled at the periphery of the compressor face by a calibrated rotary valve. For the static tests, the blunted cowl lips were replaced with a bellmouth (see fig. 3).

Each nacelle was attached to the wing by two links normal to the nacelle axis, and the axial force was measured by a load cell attached to the wing (see fig. 2). An accelerometer in the nacelle allowed the load cell to be compensated for axial acceleration. The axial force transmitted to the compensated load cell can be divided into two parts: (1) nacelle drag forward of the research nozzle, referred to as the tare force and (2) research nozzle gross thrust minus drag. Gross thrust minus drag is determined by adding the tare force to the compensated load cell reading

The tare force can be divided into four parts: ram drag, additive drag, pressure drag on the nacelle and strut, and friction drag on the nacelle and strut. For the static tests, of course, there is no ram drag or additive drag. Also, the pressure drag on the nacelle and strut and the friction drag are negligible. So the tare force was zero for the static tests. For the flyover tests the additive drag is zero since the mass flow ratio is greater than unity. Also, pressure drag on the nacelle and strut is negligible at the low flight speed of the present test. Thus, the tare force was determined, in a manner similar to reference 3, to be the sum of the ram drag plus the skin friction drag on the nacelle and strut.

Primary Nozzle

The variable-area primary exhaust nozzle is made up of overlapping leaves that provide a nearly circular throat. The leaves translate on a roller-track-cage arrangement, causing a change in the nozzle convergence angle (fig. 4).

Exhaust Nozzles

The three exhaust nozzles selected for this program were a cylindrical ejector, an auxiliary inlet ejector, and a plug nozzle. The geometric characteristics of the three exhaust nozzles are given in table I for primary nozzle settings of military and maximum afterburner power.

The cylindrical ejector nozzle is shown in figure 5. It had been used previously to determine the tare force and had a blunt base. (The blunt base was used so that the

external pressure drag could very accurately be determined.) Further details of the cylindrical ejector are given in reference 4. For an ejector nozzle of this type, to be suitable for supersonic cruise aircraft, would require a boattail surface similar to that shown by the dashed lines in figure 5.

The auxiliary inlet ejector nozzle is presented in figure 6. The nozzle incorporates a series of 16 auxiliary inlet doors located around the periphery of the external skin ahead of the primary nozzle. The principal purpose of the doors is to allow outside air to enter the ejector, which helps reduce the overexpansion of the primary jet at takeoff conditions. The present configuration had the doors fixed in the 16° position. The aft portion of the nozzle simulated the closed position. This position for the doors and the aft part of the nozzle are characteristic of low-pressure-ratio operation. Additional details of this nozzle design are given in reference 5.

The plug nozzle configurations are shown in figure 7. At the military power setting the configuration consisted of an uncooled plug and a primary flap with a 14° trailing-edge angle. At maximum afterburner power, a cooled plug body was used. It was convectively cooled along 60 percent of its length using compressor discharge air, which was then discharged through an annulus at the 60 percent location. The remainder of the plug was film cooled with the discharged air. This configuration had a primary flap with a 7.57° boattail angle. A plug nozzle generally has a translating outer shroud, which, for efficient operation at low speeds, is retracted. The present configurations simulate the shroud in this position. Further details concerning both the uncooled and cooled configurations are given in references 6 and 7, respectively.

Instrumentation

An onboard digital data system was used to record pressures, temperatures, and load cell output on magnetic tape. It had the capability of recording 578 parameters in 11.6 seconds (ref. 3). A flight calibrated test boom located on the aircraft nose was used to determine free-stream static and total pressure, aircraft angle of attack, and yaw angle. Aircraft altitude was determined using an onboard radio altimeter and a barometric altimeter along with ground-based radar. This resulted in determining the altitude to within ±3 meters (10 ft). Aircraft speed was obtained from a calibrated Mach meter. The output of the Mach meter was sampled and recorded six times in about 11.6 seconds by the onboard digital data system. The standard deviation of the estimated overall accuracy of the measurement (Mach meter plus data system) is about ±1.4 meters per second (4.5 ft/sec).

Engine airflow was determined using the calibration results from reference 8 along with measurements of engine speed and total pressure and temperature at the compres-

sor face. Fuel flows were obtained from calibrated flowmeters. Total temperature T_8, total pressure P_8, and effective area A_8 at the primary nozzle exit were obtained by using the values of engine airflow and fuel flow, the measured values of total pressure and temperature at the turbine discharge, and afterburner temperature rise and pressure drop calibration results from reference 8. Calibration of the secondary flow valve pressure drop and position were used to determine secondary airflow.

Total pressure and temperature of the secondary air were obtained from probes (fig. 8). For the ejector nozzles the probes were located beneath the primary nozzle housing at 0°, 90°, 180°, and 270° (fig. 8(a)). For the plug nozzles, the probes were located near the exit of the secondary flow passage (fig. 8(b)). The thermocouples were chromel-alumel and had radiation schields.

The noise measuring instrumentation used in these tests is shown in the block diagram of figure 9. For the flyover tests a primary and backup microphone were used, both were of the 2.54-centimeter (1-in.) diameter ceramic type. The flyover results in this report were recorded using the primary microphone. For the static tests only the primary microphone was used. Frequency response of the microphones was flat to within ±2 decibels for grazing incidence over the frequency range used. The outputs of the microphones were recorded on a two-channel direct-record tape recorder. The entire system was calibrated for sound level in the field before and after each test with a conventional tone calibrator. The tape recorder was calibrated for linearity using a "pink" noise (constant energy per octave) generator.

The flyover signal recorded on magnetic tape was played back through one-third-octave band filters and then reduced to a digital form (see fig. 9(b)). The averaging time used for data reduction was 0.1 second. The digital results were recorded on a tape. (The tape would be used later in a computer program.) The time history of each flyover (in terms of perceived noise level (PNL)) and three associated frequency spectra (at peak PNL and 10 PNdB down on either side) were automatically plotted.

The static signal recorded on magnetic tape was played back through one-third-octave band filters, and the spectra were automatically plotted (see fig. 9(c)). The averaging time used during data reduction was 0.125 second. The plotted results were converted into digital form and recorded on tape.

Meteorological conditions in terms of dry-bulb and dew point temperatures, wind speed and direction, and barometric pressure were recorded periodically throughout the test. Wind speeds were less than 5.144 meters per second (10 knots) during the tests.

Procedure

The static data for the auxiliary inlet ejector nozzle and the cylindrical ejector nozzle used in this report were obtained from an isolated nacelle (previously reported in

ref. 1). Static data for the plug nozzle was obtained with the nacelle mounted on the aircraft.

The microphone stations for the acoustic measurements at static conditions are shown in figure 10(a). The measurements were made at a radial distance of 30.5 meters (100 ft) from the nozzle exit in increments of 10° over a 90° sector. The portable microphone was positioned 1.22 meters (4 ft) above the concrete surface and was oriented to receive the acoustic pressure waves at normal incidence (fig. 10(b)). It was fitted with a wind screen that caused no loss of signal. During the measurements, the main J75 engine was at idle. The J85 in the nacelle containing the research nozzle was operated over a range of power settings, and the J85 engine in the other nacelle was shut off.

Background noise level for the static tests was determined with both J85 engines shut off, the J75 engine at idle, and external cooling air on. It was necessary to supply air from an external source to cool the J85 engine when it was operating at the military power setting. The air was supplied from an air start cart which was located on the far side of the aircraft (fig. 11). The supply line went from the start cart to the J85 engine, and the air was directed around the engine through a nozzle (see fig. 3). The J75 engine had to be operating when static data were taken because it supplied the electrical power for the onboard digital data system.

The spectra with the J75 engine at idle and with the external air on are given in reference 2 (adjusted to standard day). The spectra of particular interest are those at acoustic angles of 30°, 40°, and 50°. (See fig. 12.) The spectra at each of these acoustic angles are very similar in shape and level. For the acoustic angle of 40°, the level gradually increases to about 90 decibels at 1000 hertz. It remains fairly constant at this level until at a frequency of 2500 hertz it starts to decrease and reaches a level of about 80 decibels at a frequency of 10 000 hertz. These levels are sufficiently low so they do not interfere with the noise of the research nozzle.

Acoustic measurements of the flyover noise were made from a ground station directly under the flight path. The location of the station at Selfridge Air National Guard Base is shown in figures 13 and 14. The primary microphone was positioned 1.22 meters (4 ft) above the concrete surface, and the backup microphone was positioned 2.54 cm (1 in.) off the concrete surface. The primary microphone was fitted with a wind screen that caused no loss of signal. The microphone setup is shown in figure 15. Both microphones were oriented to receive the acoustic pressure waves at grazing incidence.

The flyovers were conducted at Mach 0.4 and at an altitude of 91.4 meters (300 ft). (The selection of this altitude will be discussed later.) The main engine of the aircraft was at idle power while the data were being recorded. The J85 engine in the nacelle that contained the research nozzle was operated at the military or maximum afterburner power setting. The J85 engine in the opposite nacelle was shut off and allowed to windmill.

As the aircraft travels along its flight path, the direct ray distance from the nozzle to the microphone R_p continuously changes (see fig. 16(a)). The angle between the direct ray and the jet exit centerline, referred to as the acoustic angle θ, also changes (see fig. 16(a)). By the time the sound has reached the microphone, however, the aircraft has moved to a new location. The ground distance between this new location and the microphone is shown in figure 16(b) as a function of θ. The values of R_p, θ, and ground distance are related to the sound data taken at a particular instant of time by having a ground observer manually record a 400-hertz signal on the tape (see fig. 9) as the aircraft passes directly over the microphone (i.e., at a ground distance of zero). The overall position accuracy is estimated to be within ±12.2 meters (40 ft) throughout the flyover.

The background noise level during flyover was determined with the main engine at idle power and both J85 engines shut off and allowed to windmill. The results are shown in figure 17 in terms of the variation in PNL with ground distance. The noise level increases as the aircraft approaches the microphone and reaches a peak value of 102 PNdB at a ground distance of about zero. The noise level then decreases to 96.5 PNdB at a ground distance of 100 meters (328 ft). A ground distance of 100 meters, as will be shown later, is about where the research exhaust nozzles reach their peak noise levels.

The frequency spectra at both the peak background noise level and the noise level corresponding to the ground distance of 100 meters (328 ft) are shown in figure 18. The levels for both spectra are fairly constant over most of the frequency range. For the spectrum associated with the peak background noise (fig. 18(a)), the level is about 75 decibels at frequencies less than 4000 hertz. At higher frequencies, the level decreases to a value of about 60 decibels at 10 000 hertz. For the spectrum associated with the noise level at a ground distance of 100 meters (fig. 18(b)), the level is about 70 decibels at frequencies below about 2000 hertz. At higher frequencies, the level also decreases to a value of about 60 decibels at 10 000 hertz. These levels are sufficiently low so they do not interfere with the noise from the research nozzles.

As mentioned, the J85 engine in the nacelle containing the research nozzle was operated at either the military or maximum afterburner power setting, and the J85 engine in the opposite nacelle was allowed to windmill. This asymmetric power setting resulted in yaw angles for the aircraft of only about 1°. The yaw angle was maintained at this small value by using some elevon to put the aircraft in a slight bank. The resulting increase in the scrubbing noise over the elevon surfaces is considered insignificant compared with the increase that would result from a highly yawed aircraft.

RESULTS AND DISCUSSION

Acoustic Characteristics

Flyover altitude. - Flyover tests typically have been conducted at altitudes of about 300 meters (1000 ft) (refs. 9 and 10). The higher the altitude, of course, the longer the propagation distance from the noise source to the microphone. This, in turn, imposes increasingly severe requirements on the recording system, which make it difficult to obtain useful noise data. Based on this consideration, it would be desirable to conduct the tests at a low altitude. But it is also necessary that the altitude be high enough to be consistent with safe operation of the aircraft. This is especially important since, as mentioned, the noise data were taken while the main engine of the aircraft was at idle power.

To determine a reasonable compromise in altitude, flyovers were conducted at altitudes of 366, 183, and 91 meters (1200, 600, and 300 ft). Typical results of the variation in perceived noise level with ground distance are shown in figure 19. The data are for the cylindrical ejector nozzle at the maximum afterburner power setting. At the highest altitude the data scatters too much to give useful results. Decreasing the altitude to 183 meters (600 ft) reduces the scatter, but it is still difficult to define accurately the peak perceived noise level or where it occurs. An altitude of 91 meters (300 ft) provides acoustic data that are repeatable to within ±1.5 PNdB. This altitude was selected for conducting the flyover tests.

Noise level and directivity. - The results of the flyover tests conducted at an altitude of 91 meters (300 ft) are shown in figure 20 for all of the nozzles tested. The results are presented in terms of the variation in perceived noise level as a function of ground distance. Figure 20(a) shows the results for military power setting. The noise level of the uncooled plug nozzle increases as the aircraft approaches the microphone. It continues to increase as the aircraft passes directly over the microphone. A peak level of 122 PNdB is reached at a ground distance of 92 meters (301 ft). The noise remains at this level until the aircraft has receded to a ground distance of 170 meters (559 ft) after which it falls off.

The noise levels of the cylindrical ejector and auxiliary inlet ejector nozzles also reach their peak values after the aircraft has passed well overhead and is receding from the microphone. The cylindrical ejector reaches a peak level of 122 PNdB at a ground distance of 124 meters (407 ft). The auxiliary inlet ejector is the quietest of the three nozzles achieving a peak value of 119 PNdB at a ground distance of 167 meters (549 ft).

The ground distance at which the peak noise level occurs is related to the acoustic angle at which the peak noise is emitted (see fig. 16). The value of this acoustic angle is also shown in figure 20(a). For the plug nozzle, which has a fairly flat peak, this angle

extends between 37° and 59°. For the cylindrical ejector, the peak noise occurs at 45°, which is somewhat farther from the jet axis than the 40° angle associated with the auxiliary inlet ejector.

The results for maximum afterburner power are shown in figure 20(b). The noise levels of all the nozzles increase rapidly to peak values. The cooled plug reaches the highest peak level (131 PNdB) at a ground distance of 126 meters (413 ft), corresponding to an acoustic angle of 48°. The cylindrical ejector has a peak level of 127 PNdB at a ground distance of 109 meters (359 ft). The acoustic angle is 55°. The auxiliary inlet ejector again is the quietest with a peak level of 126 PNdB occurring at a ground distance of 88 meters (290 ft). Its acoustic angle of 57° is the farthest from the jet axis of the three nozzles.

Comparison with SAE prediction. - In addition to determining the peak noise levels of these nozzles and the angle at which they occur, it is also important to determine if the SAE method (ref. 11) adequately predicts the peak flyover noise spectra. One of the important reasons for predicting the spectra is to enable perceived noise levels to be estimated. A comparison of measured and predicted sound pressure levels for peak flyover noise is presented in figures 21 and 22 along with the values of perceived noise level in PNdB and the overall sound pressure level in decibels. Figure 21 presents the results for nominal military power. For the uncooled plug nozzle (fig. 21(a)) the predicted sound pressure level was somewhat higher than the measured level for frequencies above 500 hertz. Even so, this resulted in overestimating the perceived noise level by only about 2.5 PNdB. The estimated value of the overall sound pressure level was about the same (1.3 dB higher) as the predicted value. For both the cylindrical ejector and the auxiliary inlet ejector nozzles (fig. 21(b) and (c)), the predicted values of sound pressure level were higher than the measured values for all except the low frequencies. This resulted in overestimating the perceived noise level of the cylindrical ejector by about 4 PNdB and the overall sound pressure level by about 4 decibels. The greatest difference between estimated and measured levels occurred for the auxiliary inlet ejector. The perceived noise level was overestimated by about 7 PNdB, and the overall sound pressure level by about 6 PNdB.

Figure 22 presents the results for maximum afterburner power. For the cooled plug (fig. 22(a)) the predicted values of sound pressure level were higher than the measured values for frequencies above about 250 hertz. This resulted in overestimating the perceived noise level by about 3 PNdB and the overall sound pressure level by about 3 decibels. The differences between the estimated and measured PNL and overall sound pressure level (OASPL) for the cylindrical ejector (fig. 22(b)) and the auxiliary inlet ejector (fig. 22(c)) were about the same, 8 PNdB and 6 dB, respectively.

Flight velocity effects. - As mentioned, the flyover tests were conducted at Mach 0.4, and the results showed the plug nozzle to be the noisiest and the auxiliary inlet ejector nozzle to be the quietest. Flyover predictions based on static results (ref. 1), how-

ever, indicated that the plug should be the quietest and the auxiliary inlet ejector the noisiest at military power. This reversal could be due to the effect of flight velocity.

To investigate this, the approach was to adjust the measured flyover and static spectra to comparable conditions, which were 30.48 meters (100 ft) from the nozzle in the free field and on a standard day. A substantial adjustment was applied to the amplitude of the static spectra of an auxiliary inlet ejector nozzle (AIE) and a cylindrical ejector nozzle in the midfrequency range. This was necessary to remove the effect caused by taking the data over a grassy surface rather than a concrete surface. The adjustment was shown to give good agreement for data from a cylindrical ejector nozzle that was tested over both surfaces. Details of all adjustments are given in the appendix. The comparison was then made at a constant relative jet velocity and acoustic angle.

In making the comparison, the greatest emphasis should be placed on the data at frequencies between 160 and 5000 hertz. At frequencies below 160 hertz, the short integration time, the rapidly changing conditions of the flyover, and the narrowness of the frequency bands combine to give results that are unreliable. Above 5000 hertz the acoustic signal received at the ground station quite possibly is below the noise floor of the recording equipment (ref. 12). Values of the atmosphermic absorption coefficient are very large at these high frequencies and multiply the noise floor to unrealistically high noise levels in correcting the data to 30.48 meters (100 ft).

Comparison of flyover and static spectra for the uncooled plug nozzle is presented in figure 23 for the three acoustic angles θ at which the flyover noise was near its peak value and for a relative jet velocity V_R of 600 meters per second (1970 ft/sec). At an acoustic angle of 30° (fig. 23(a)) and for a frequency of 160 hertz, the sound pressure level value for the flyover spectra is about 11 decibels below that of the static spectra. At higher frequencies the differences between the spectra become smaller. (The sharp dip in the flyover spectra at 400 Hz is probably due to ground interference. Theory indicates that a second dip would be expected to occur at about this frequency.) This resulted in an OASPL value that was $2\frac{1}{2}$ decibels lower and a PNL value that was about $1\frac{1}{2}$ PNdB lower for the flyover spectrum than for the static spectrum. As the acoustic angle increases to 40° (fig. 23(b)) and then to 50° (fig. 23(c)), the agreement between the spectra is very good. There is no significant difference in either the OASPL or the PNL values between the static and the flyover spectra.

The comparison of the flyover and static spectra for the cylindrical ejector is shown in figure 24. The trend of closer agreement between the flyover and static spectra as the acoustic angle increases also is evident for this nozzle. Again, the OASPL value and the PNL value are lower for the flyover spectra than for the static spectra, although the magnitude of the differences is somewhat larger than for the uncooled plug nozzle.

The comparison of the flyover and static spectra for the auxiliary inlet ejector nozzle is shown in figure 25. The trend of closer agreement between spectra as the acoustic angle increases is not evident. In fact, the opposite trend occurs. Also, the magnitude

of the differences between flyover and static spectra is considerably greater at acoustic angles of 40° and 50° than for the other two nozzles. At an acoustic angle of 40°, the OASPL and PNL values were 9.4 decibels and 7.5 PNdB lower for the flyover than for the static spectra. At an acoustic angle of 50°, the OASPL and PNL values were 10.0 decibels and 10.7 PNdB lower for the flyover than for the static spectra. This suggests a significant flight velocity effect on the auxiliary inlet ejector nozzle compared with the other two nozzles. It is partly caused by a difference in the amount of outside air that enters the ejector through the auxiliary inlet doors at flyover conditions compared with static conditions.

Another indication of the flight velocity effect is the directivity of the noise. Comparison of flyover and static noise directivity is shown in figure 26. For the plug nozzle the static and flyover noise follow the same trend with changes in the acoustic angle. The same is true for the cylindrical ejector nozzle. For the auxiliary inlet ejector nozzle, however, the static and flyover noise follow opposite trends. The static results show the noise level increasing with increasing acoustic angle, and the flyover results show the noise level decreasing with increasing acoustic angle. This accounts, in part, for the flyover noise being less than predicted from static results since the aircraft was farther away than predicted when the peak noise was received by the microphone.

Thrust Characteristics

So far the discussion has been concerned with the acoustic characteristics of the nozzles. Equally important are their thrust performance characteristics. A comparison of thrust performance characteristics, in terms of nozzle gross thrust coefficient, is presented in figure 27. Results are shown for flyover conditions at both military and maximum afterburner power settings. Also included is a comparison of the peak noise levels of the nozzles as a function of relative jet velocity. Peak noise is given in terms of perceived noise level normalized by subtracting the term $10 \log_{10} \rho^2 A$ (ref. 11).

As shown (and as already mentioned in connection with fig. 20), the auxiliary inlet ejector nozzle was the quietest and the plug nozzle the noisiest at both military and maximum afterburner power settings. The difference is about 4 PNdB at military power and about 5 PNdB at the maximum afterburner power setting. The cylindrical ejector nozzle was about 3 PNdB noisier than the auxiliary inlet ejector nozzle at military power and about the same noise level as the auxiliary inlet ejector at the maximum afterburner power setting.

The auxiliary inlet ejector was not only the quietest nozzle tested but also the highest in thrust performance. Thrust performance is given in terms of nozzle gross thrust coefficient. At military power the performance of the auxiliary inlet ejector nozzle was

about 2 percentage points higher than that of the plug nozzle, 0.985 compared with 0.965. At maximum afterburner power they had about the same performance, 0.980. But, it should be noted that about 4 percent of the J85 engine airflow was bled from the compressor discharge to cool the plug at the maximum afterburner power operation. The cylindrical ejector nozzle had the lowest performance at both power settings. At military power setting the large internal expansion ratio, d_9/d_8 caused the primary jet to be considerably overexpanded resulting in a nozzle gross thrust coefficient of 0.890. (Although the auxiliary inlet ejector also has a large value of d_9/d_8, the external air entering the ejector through the auxiliary inlet doors helped keep the primary jet properly expanded.) Going to maximum afterburner power setting reduces the internal expansion ratio, which reduces the overexpansion of the primary jet, and the nozzle gross thrust coefficient increases to 0.935.

SUMMARY OF RESULTS

A series of flyover tests were conducted at an altitude of 91 meters (300 ft) and at Mach 0.4 on a plug nozzle, an auxiliary inlet ejector nozzle, and a cylindrical ejector nozzle. The primary jet exhaust was provided by a calibrated afterburning turbojet engine. Data were taken at the military and maximum afterburner power settings, which resulted in relative jet velocities of 500 and 860 meters per second (1640 and 2820 ft/sec). The results may be summarized as follows:

1. A flyover altitude of 91 meters (300 ft) provided acoustic data that was repeatable to within ±1.5 perceived noise decibels (PNdB).

2. Flight velocity appeared to reduce the noise of an auxiliary inlet ejector nozzle. This is based on a comparison of static and flyover spectra after a number of adjustments had been made to bring the measured spectra to similar conditions.

3. The auxiliary inlet ejector nozzle was the quietest in flyover, and the plug nozzle the noisiest; the difference was 4 PNdB at military power and 5 PNdB at maximum afterburner power.

4. Sound pressure levels predicted by SAE were somewhat higher than the measured levels. This resulted in overpredicting both the overall sound pressure level and the perceived noise level. The closest agreement was for the plug nozzle where the predicted value of perceived noise level was within 3 PNdB of the measured value. The greatest disagreement was for the auxiliary inlet ejector nozzle where the predicted value of perceived noise level was 7 PNdB larger than the measured value.

5. At military power, the performance (in terms of nozzle gross thrust coefficients) of the auxiliary inlet ejector nozzle was about 2 percentage points higher than the uncooled plug, 0.985 compared with 0.965. At maximum afterburner power they had about the same performance. 0.980. The cylindrical ejector had the lowest performance at both power settings, 0.890 at military and 0.935 at maximum afterburner.

Lewis Research Center,
National Aeronautics and Space Administration,
Cleveland, Ohio, April 30, 1973,
501-24.

APPENDIX - ADJUSTMENTS TO MEASURED SPECTRA

To determine whether differences exist between the flyover and the static data, the measured spectra were adjusted to comparable conditions of 30.48 meters (100 ft) from the nozzle in the free field and on a standard day of 25° C (77° F) and 70 percent relative humidity. The standard day adjustment was made using the simplified procedure of Federal Air Regulation (FAR)36 (ref. 13). The adjusted flyover and static spectra would then be directly comparable. Details of the adjustments are presented here.

Static

Static data for both ejector nozzles (cylindrical ejector and auxiliary inlet ejector) were taken with an isolated nacelle over a grassy surface, and data for the plug nozzle were taken on the aircraft over a concrete surface. Each required a different method to make the free-field adjustment. The adjustment from concrete to free field was based on the assumption that the concrete surface was a perfect reflector and that the jet noise was a single point source (ref. 14). The theoretical correction is shown in figure 28(a). For jet noise, however, there are many noise sources distributed over a significant length of the jet. This has the effect of reducing the magnitude of the theoretical correction. Consequently, the theoretical curve was modified by a smooth curve tangent to the theoretical curve at the low and high frequencies as shown in the figure. This gross adjustment amounted to reducing the magnitude of the spectra by about 6 decibels at the low frequencies and 3 decibels at the high frequencies.

The adjustment from grass to free field was done by first adjusting the data from grass to concrete and then adjusting it from concrete to free field. The adjustment from concrete to free field has just been described. The adjustment from grass to concrete was based on data from a cylindrical ejector nozzle that was tested over both surfaces. The spectra are shown in figure 28(b). There was a large difference only in the midfrequencies. Therefore, the spectrum taken over grass was adjusted to that taken over concrete by connecting the lower and upper segments of the measured spectrum by a smooth curve of the same shape as that predicted by SAE. The resulting OASPL and PNL values for the spectrum adjusted grass to concrete are about the same as those for the spectrum taken over concrete. This adjustment from grass to concrete was applied to both ejector nozzles (cylindrical and auxiliary inlet ejectors). It was assumed that the spectral shape of both nozzles is very similar. This adjustment did not need to be made to the plug nozzle since it was tested over a concrete surface.

Further evidence of the validity of the adjustment from grass to concrete is shown in figure 28(c). Here, the results for a plug nozzle tested over a concrete surface are com-

pared with that of a similar nozzle tested over a grassy surface (from ref. 1). The spectra adjusted in both cases to free field and standard day by these procedures are compared in the figure. There is good agreement between the spectra except in the vicinity of 200 and 1600 hertz. The reason for the dip at 200 hertz is not yet known, but the dip at 1600 hertz is attributed to destructive interference of the concrete surface. The resulting OASPL and PNL values for the spectra are within 2 decibels of each other.

The last adjustment was for microphone orientation. The static data were taken with the microphone oriented to receive the acoustic waves at normal incidence. The data were adjusted to that obtained if the microphone had been oriented for grazing incidence to obtain the actual sound pressure level values. The adjustment resulted in reducing the amplitude of the static spectrum at frequencies above 2000 hertz, varying from 0.1 decibel at 2500 hertz to 4 decibels at 10 000 hertz.

Flyover

Ground reflection cancellation or addition is dependent on the difference in path length between the direct and reflected ray. During flyover the ray paths and the acoustic angle θ change continuously (fig. 29(a)).

Adjustments from concrete to free field for these varying conditions was done by using a ground reflection correction curve for the case where the airplane is directly overhead (fig. 29(b)). This curve was obtained in a manner similar to that for the static data. In order to apply ground reflection corrections for other positions of the aircraft, this curve was entered at a distance corrected frequency f_{DC} such that the same phase relation between the direct and reflected ray would exist as for the overhead case. This was done by correcting the frequency so that the first cancellation frequency would coincide with that for the overhead case. Since succeeding cancellation and addition frequencies are multiples, the proper phase relation would exist for all frequencies.

The distance corrected frequency parameter is derived as follows (see fig. 29(c)):

The first cancellation occurs when the difference in path length between the direct and reflected ray is equal to one half wave length. For the case of the aircraft directly overhead

$$\frac{\lambda}{2} = 2h_m$$

where λ is the wave length. The first cancellation frequency is

$$f_{10} = \frac{a}{4h_m} \tag{A1}$$

where f_{10} is the first cancellation frequency overhead case and a is the speed of sound.

For the general case the length of the reflected ray is

$$R_R = \sqrt{R_p^2 + 1200\ h_m}$$

for $H = 300$ feet. The half wave length at first cancellation frequency is then

$$\frac{\lambda}{2} = \sqrt{R_p^2 + 1200\ h_m} - R_p$$

and the first cancellation frequency is

$$f_{1g} = \frac{a}{2\left(\sqrt{R_p^2 + 1200\ h_m} - R_p\right)} \tag{A2}$$

The ratio of the first cancellation frequency for the overhead case to that for the general case is multiplied by the frequency being adjusted to obtain the distance corrected frequency.

$$f_{DC} = \frac{f_{10}}{f_{1g}} \cdot f$$

Using the values of first cancellation frequencies given in equations (A1) and (A2) results in

$$f_{DC} = F\left(\frac{\sqrt{R_p^2 + 1200\ h_m} - R_p}{2h_m}\right) \tag{A3}$$

After having been adjusted to free field and standard day conditions, the sound pressure level of a typical unsuppressed exhaust nozzle is shown in figure 29(d). The spectra were then adjusted to a constant distance of 30.48 meters (100 ft) from the exhaust nozzle. This adjustment was made accounting for inverse-square radiation and atmospheric attenuation. This resulted in increasing the spectrum level from that represented by the dashed line to that represented by the dash-dot line.

Another adjustment to the flyover data was necessary because the noise source is in motion relative to the microphone resulting in a Doppler shift of frequency. The best way to apply the Doppler shift to jet noise is not clear because the principal sources of noise are distributed over a significant length of the jet and are not all moving at the same speed. The approach used here was simply to shift all frequencies by the same amount, based on the speed of the aircraft. This amounted to shifting the frequencies by one-third-octave band at the most. Results are shown in figure 29(d).

No adjustment was made to the level of the spectrum when applying the Doppler shift. Because of the change in bandwidth, there is an adjustment to the spectrum level (ref. 15). However, the level changes less than 1 decibel for the aircraft conditions used here. According to reference 2, there is another part to the Doppler shift termed "dynamic effect." No application of the dynamic effect was made.

REFERENCES

1. Darchuk, George V.; and Balombin, Joseph R.: Noise Evaluation of Four Exhaust Nozzles for Afterburning Turbojet Engine. NASA TM X-2014, 1970.

2. Brausch, J. F.: Flight Velocity Influence on Jet Noise of Conical Ejector, Annular Plug and Segmented Suppressor Nozzles. General Electric Co. (NASA CR-120961), Aug. 1972.

3. Groth, Harold W.; Samanich, Nick E.; and Blumenthal, Philip Z.: Inflight Thrust Measuring System for Underwing Nacelles Installed on a Modified F-106 Aircraft. NASA TM X-2356, 1971.

4. Samanich, Nick E.; and Huntley, Sidney C.: Thrust and Pumping Characteristics of Cylindrical Ejectors Using Afterburning Turbojet Gas Generator. NASA TM X-52565, 1969.

5. Burley, Richard R.: Flight Investigation of Airframe Installation Effects on an Auxiliary Inlet Ejector Nozzle on an Underwing Engine Nacelle. NASA TM X-2396, 1971.

6. Samanich, Nick E.; and Chamberlin, Roger: Flight Investigation of Installation Effects on a Plug Nozzle Installed on an Underwing Nacelle. NASA TM X-2295, 1971.

7. Samanich, Nick E.: Flight Investigation of an Air-Cooled Plug Nozzle with Afterburning Turbojet. NASA TM X-2607, 1972.

8. Antl, Robert J.; and Burley, Richard R.: Steady-State Airflow and Afterburning Performance Characteristics of Four J85-GE-13 Turbojet Engines. NASA TM X-1742, 1969.

9. Coles, Willard D.; Mihaloew, John A.; and Swann, William H.: Ground and In-Flight Acoustic and Performance Characteristics of Jet-Aircraft Exhaust Noise Suppressors. NASA TN D-874, 1961.

10. Peery, H. Rodney; and Erzberger, Heinz: Noise Measurement Evaluation of Take-Off and Approach Profiles Optimized for Noise Abatement. NASA TN D-6246, 1971.

11. Anon.: Jet Noise Prediction. Aerospace Information Rep. 876, SAE, July 10, 1965.

12. Little, John W.; Miller, Robert L.; Oncley, Paul B.; and Panko, Raymond E.: Studies of Atmospheric Attenuation of Noise. NASA Acoustically Treated Nacelle Program. NASA SP-220, 1969, pp. 125-135.

13. Anon.: Federal Aviation Regulations, Vol. III, Pt. 36, Noise Standards: Aircraft Type Certification. Dept. of Transportation, Federal Aviation Administration.

14. Howes, Walton L.: Ground Reflections of Jet Noise. NASA TR R-35, 1959.

15. Mangiarotty, R.A.: Doppler Effect Correction for Motions of Source, Observer, and Fluid. Rep. D6-17095 TN, Boeing Co., 1968.

TABLE I. - NOZZLE GEOMETRIC CHARACTERISTICS

Nozzle configuration	J85 power setting	Nozzle throat effective area, A_8, m^2	Ejector exit diameter to primary nozzle exit effective diameter, d_9/d_8	Flap length spacing ratio, Le/d_8	Ejector spacing ratio, L/d_8	Nozzle throat circumference to height ratio, c/b
Cylindrical ejector nozzle	Military	0.0723	1.5	2.0	----	--
	Maximum afterburning	0.1032	1.18	1.6	----	--
Auxiliary inlet ejector nozzle	Military	0.0665	1.55	2.3	0.57	--
	Maximum afterburning	0.1052	1.28	2.0	0.55	--
Plug nozzle	Military	0.0703	----	---	----	21
	Maximum afterburning	0.1123	----	---	----	20

Figure 1. - Modified F-106B aircraft in flight.

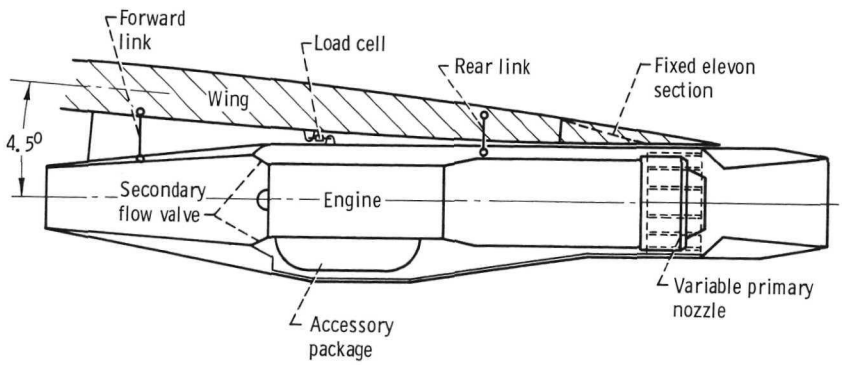

Figure 2. - Nacelle-engine installation.

Figure 3. - J85 engine installation for static tests.

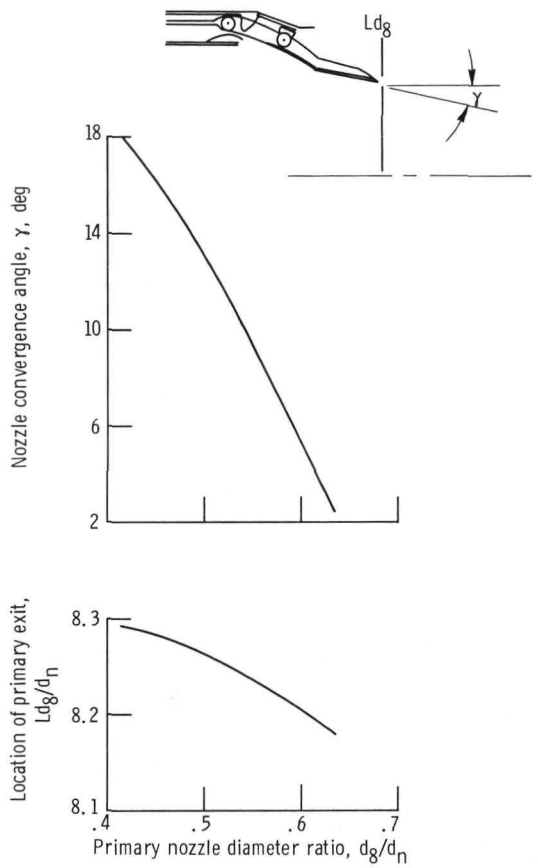

Figure 4. - Primary nozzle dimensional characteristics.

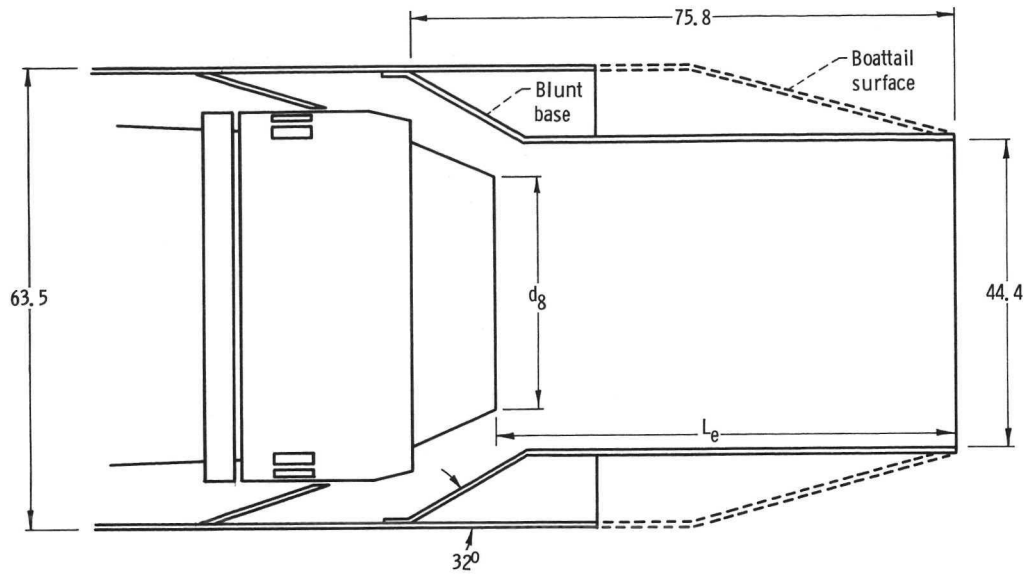

(a) Dimensional characteristics. (Linear dimensions are in cm.)

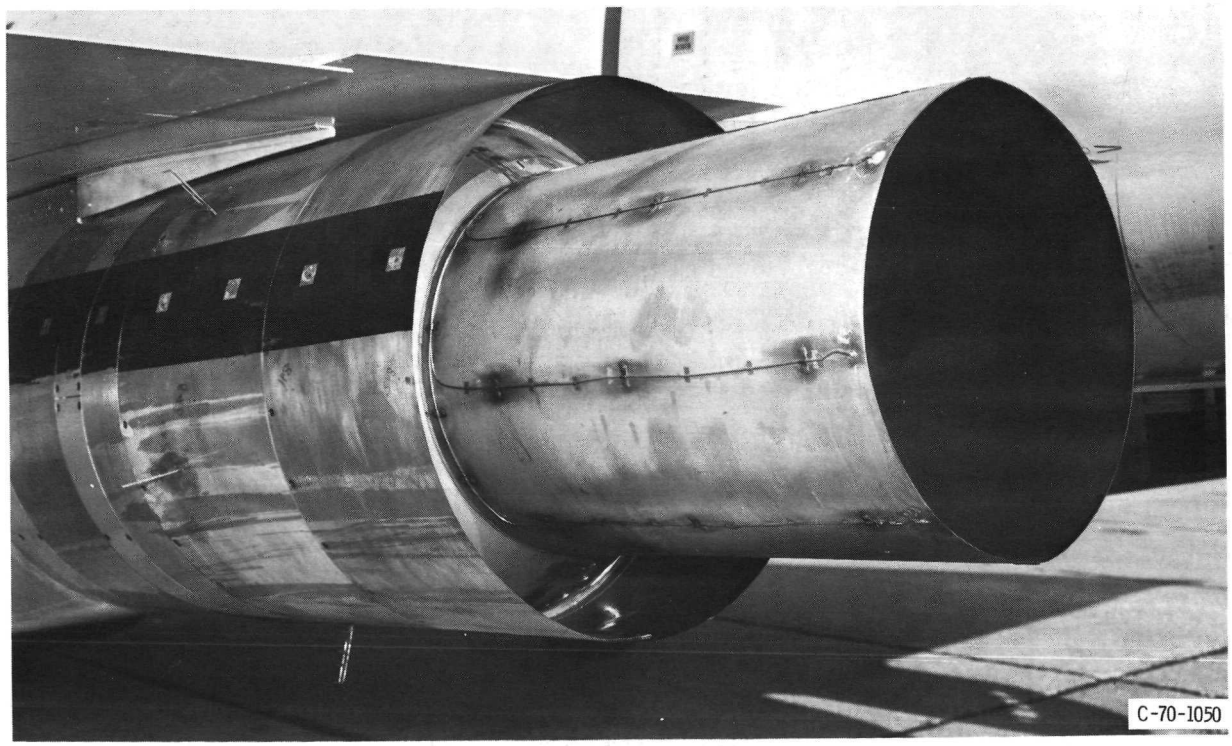

(b) Installed on aircraft.

Figure 5. - Cylindrical ejector nozzle.

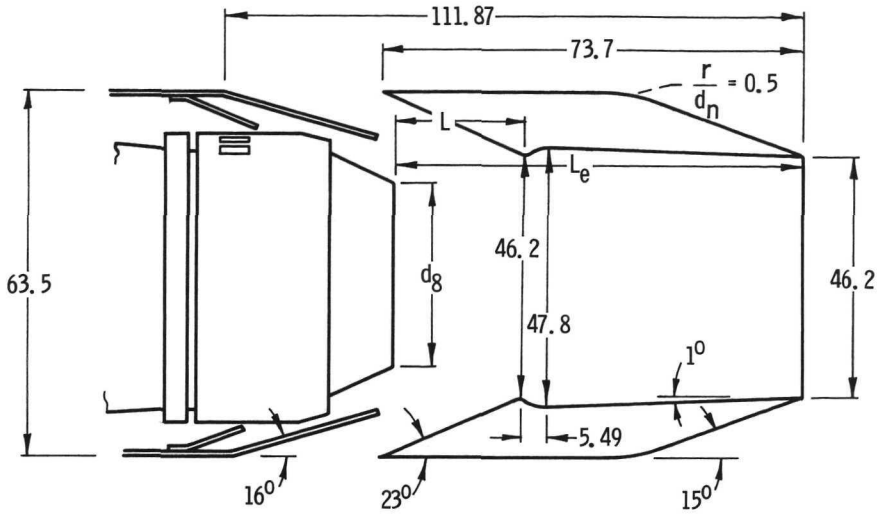

(a) Dimensional characteristics. (Linear dimensions are in cm.)

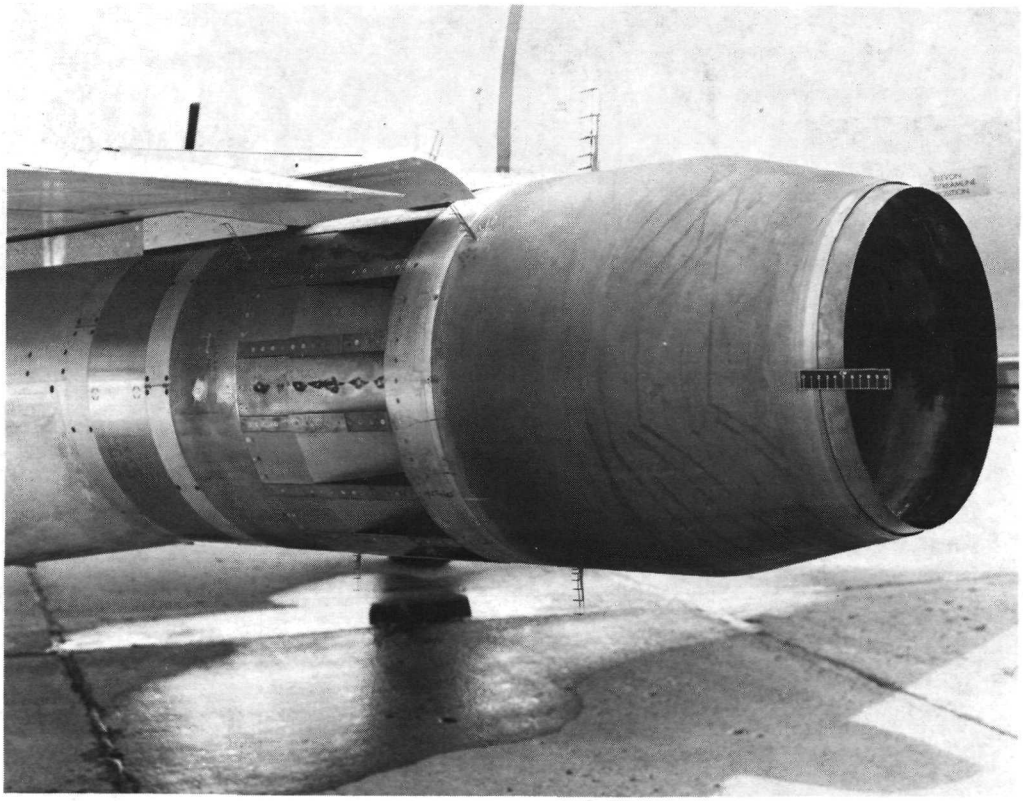

(b) Installed on aircraft.

Figure 6. - Auxiliary inlet ejector nozzle.

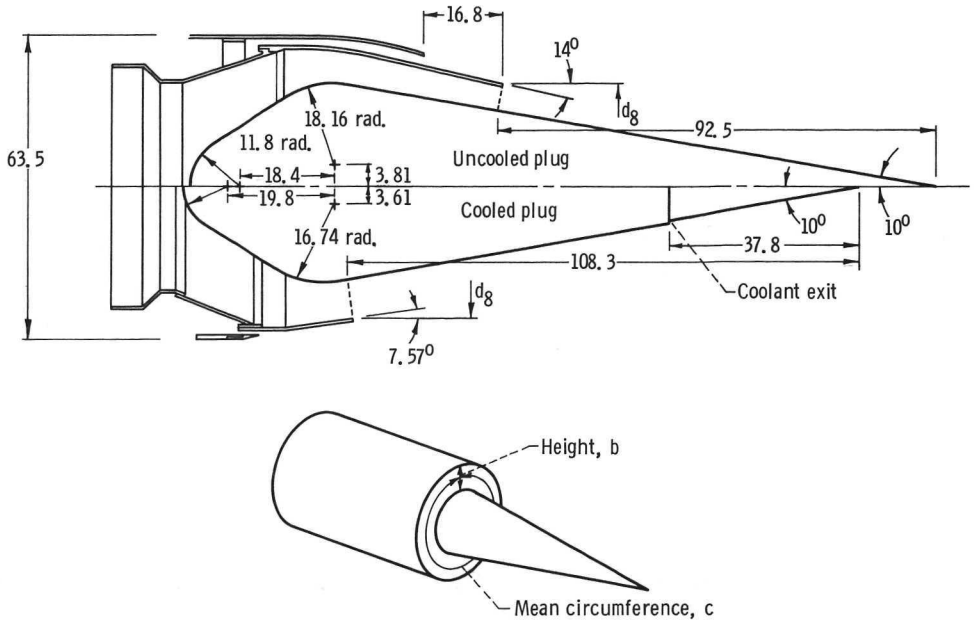

(a) Dimensional characteristics. (Linear dimensions are in cm.)

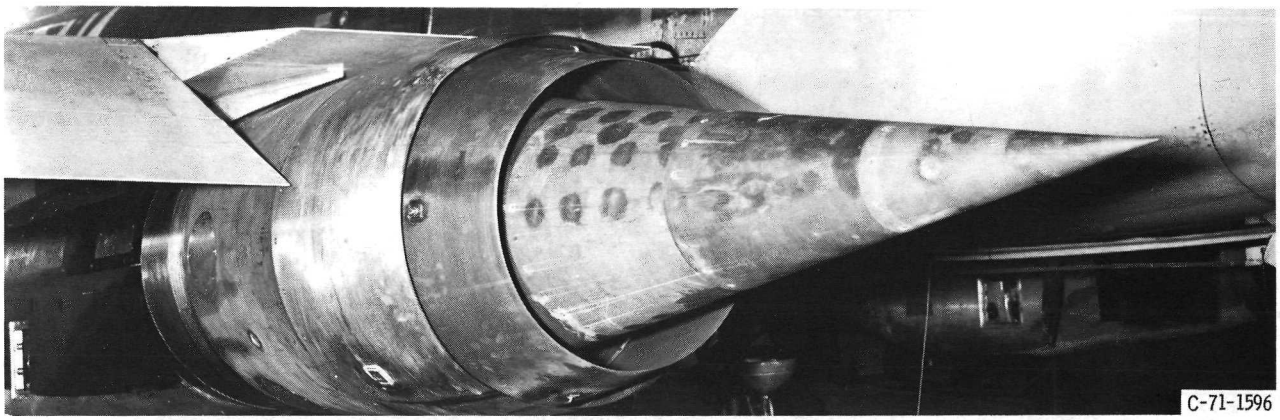

(b) Uncooled plug nozzle installed on aircraft.

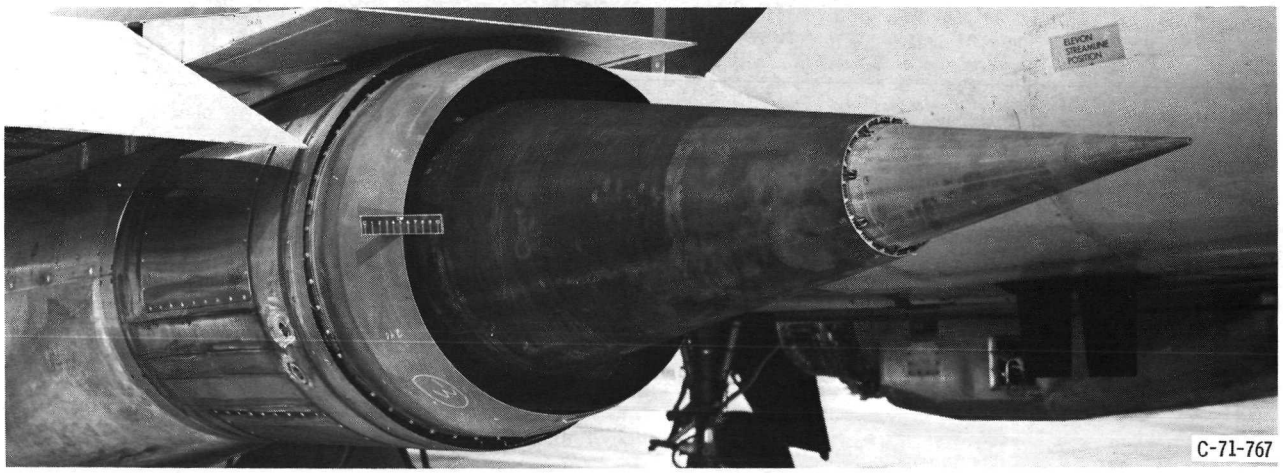

(c) Cooled plug nozzle installed on aircraft.

Figure 7. - Plug nozzle.

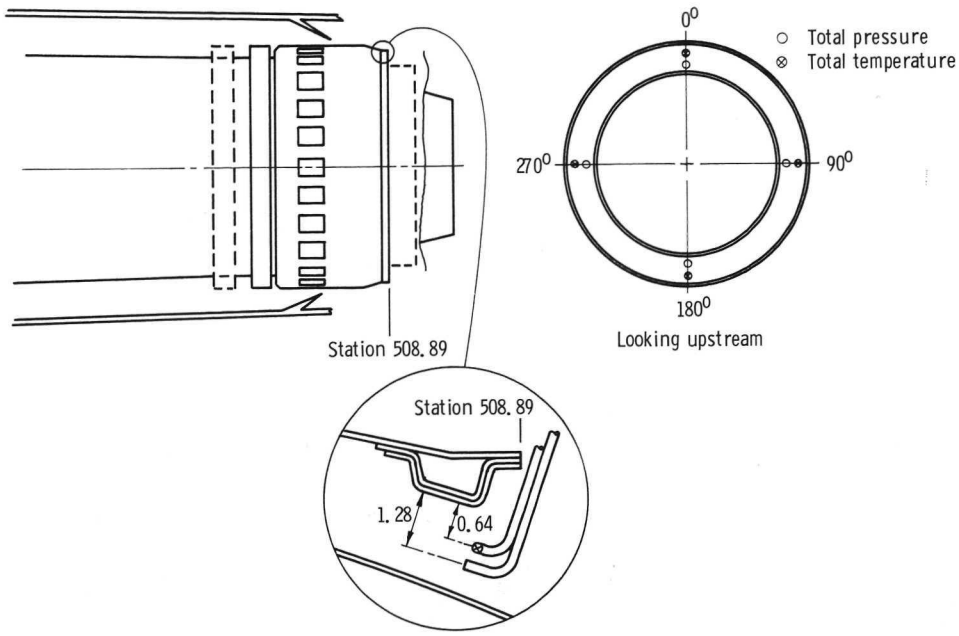

(a) Ejector nozzles.

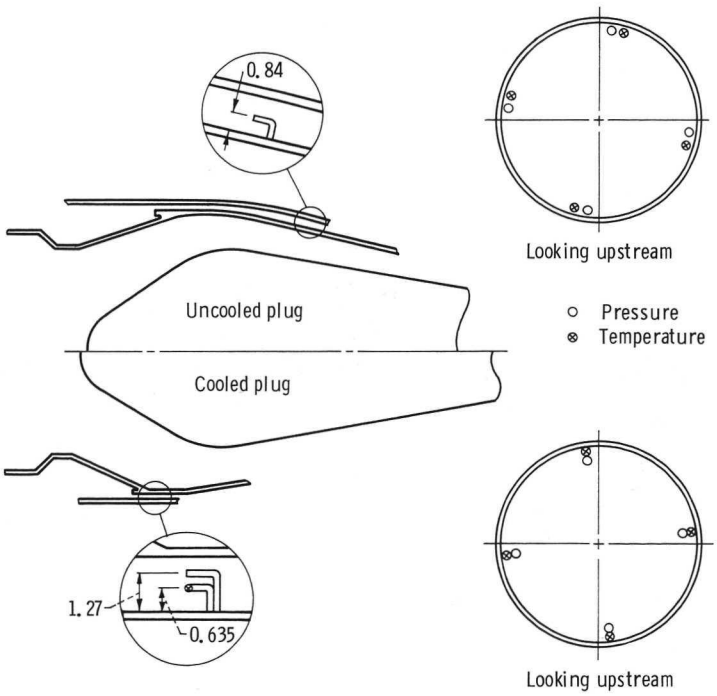

(b) Plug nozzles.

Figure 8. - Secondary passage instrumentation. (Linear dimensions are in cm.)

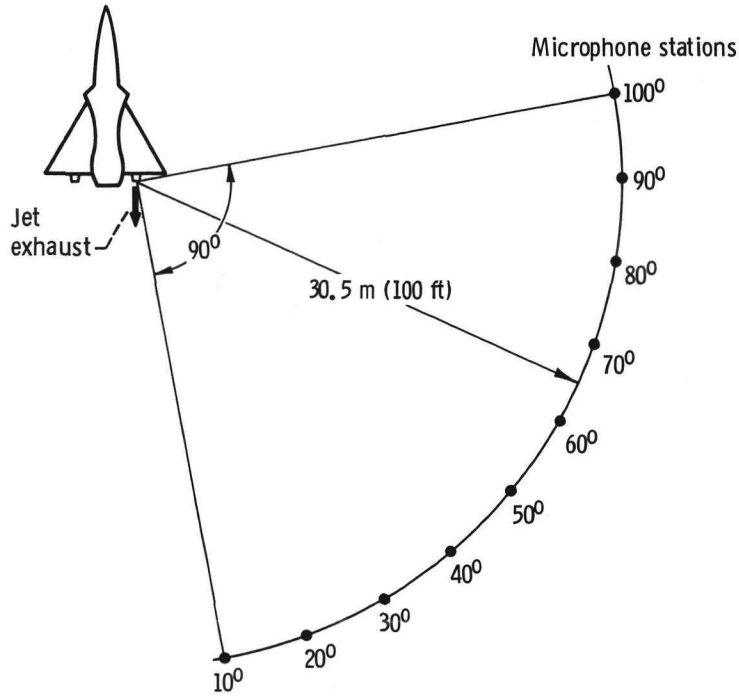

(a) Microphone stations.

(b) Microphone orientation.

Figure 10. - Microphone position and orientation for static tests.

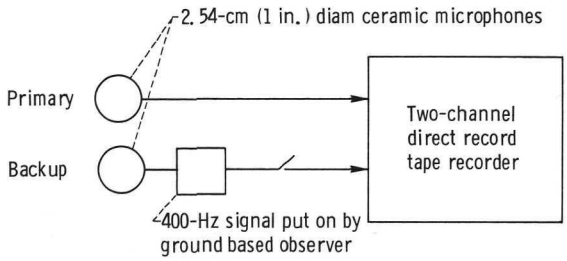

(a) Recording system.

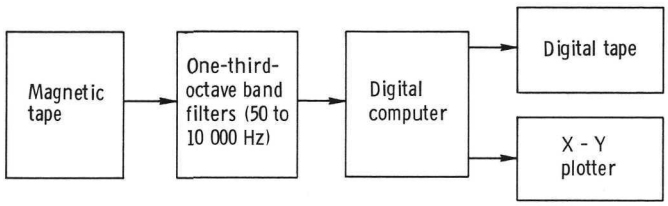

(b) Playback system for flyover data.

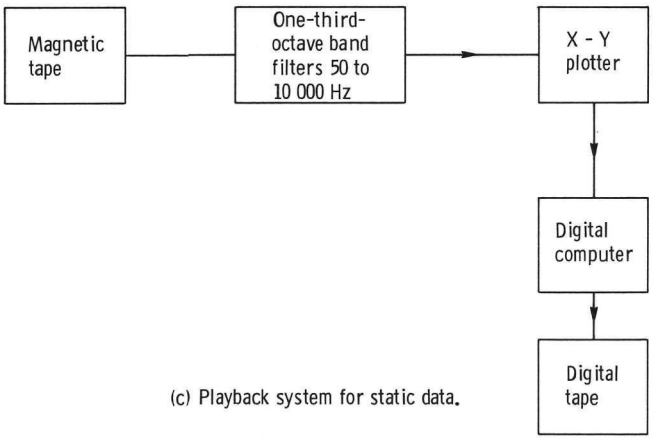

(c) Playback system for static data.

Figure 9. - Block diagram of data recording and playback system.

Figure 11. - Location of external source of cooling air for static tests.

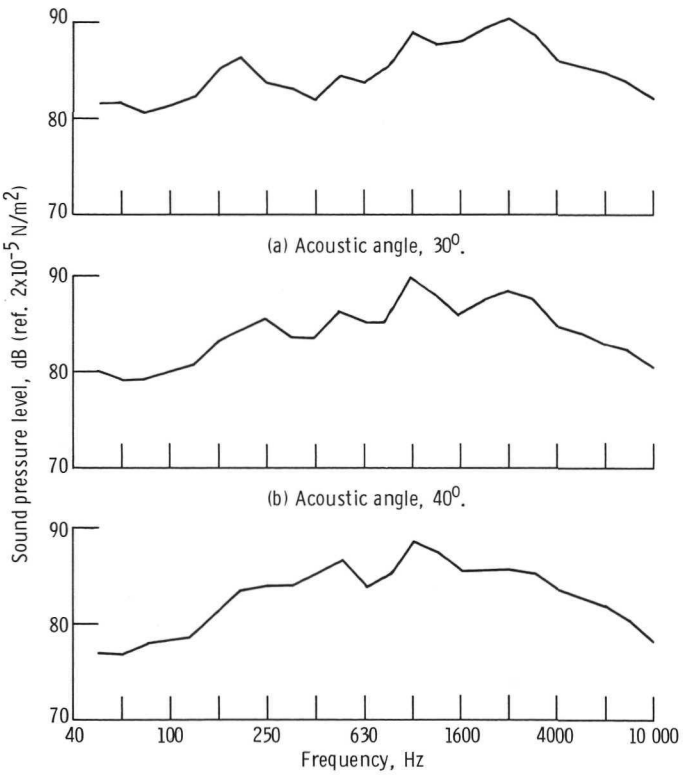

Figure 12. - Frequency spectra for background noise during static tests adjusted to standard day; one-third-octave bands.

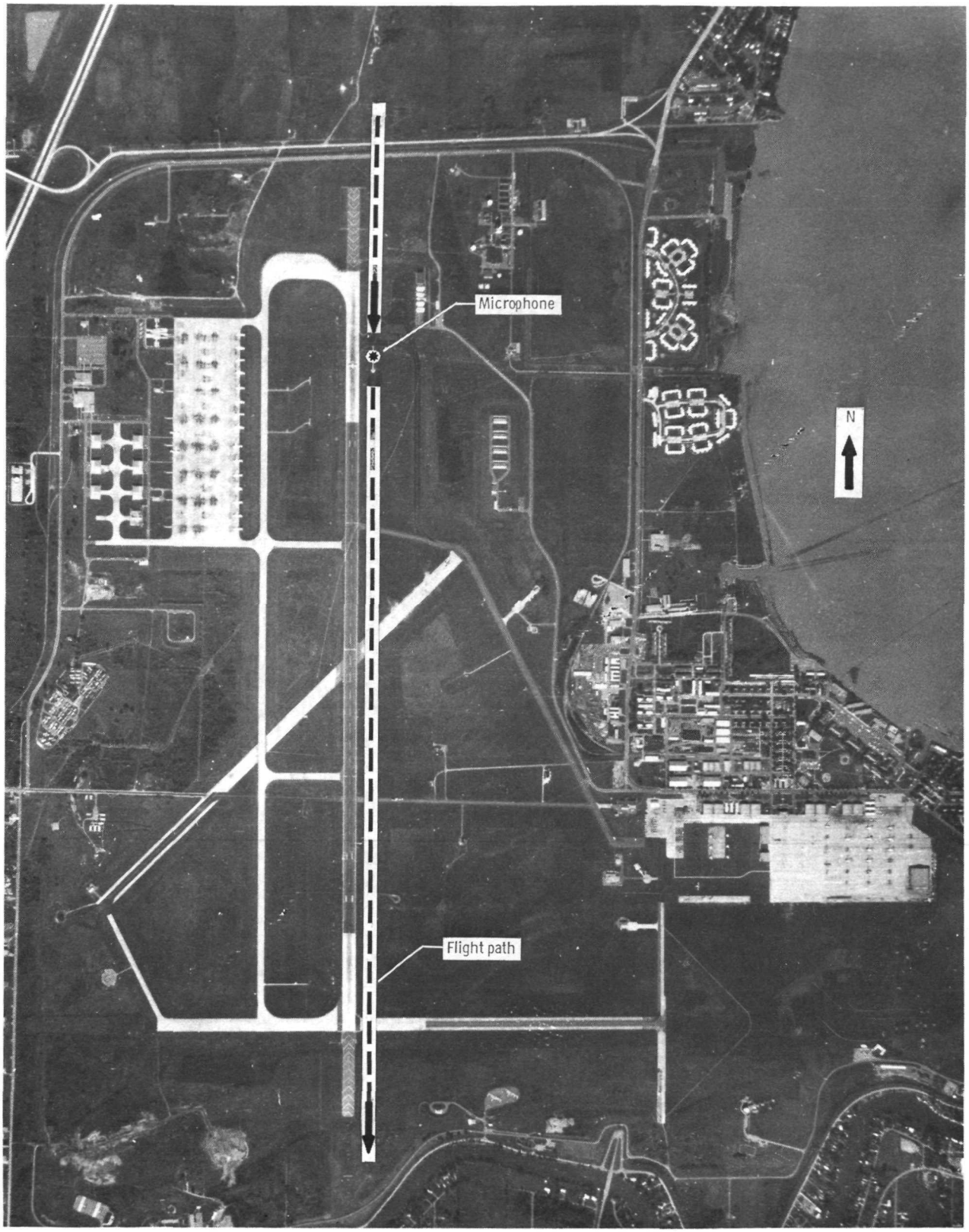

Figure 13. - Aerial photograph of Selfridge Air National Guard Base.

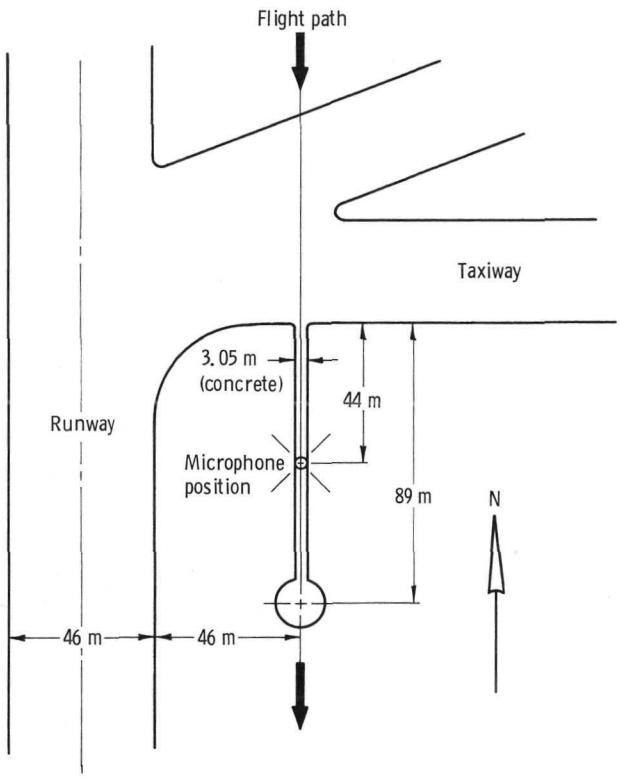

Figure 14. - Microphone position at Selfridge Air National Guard Base for sound flyover data.

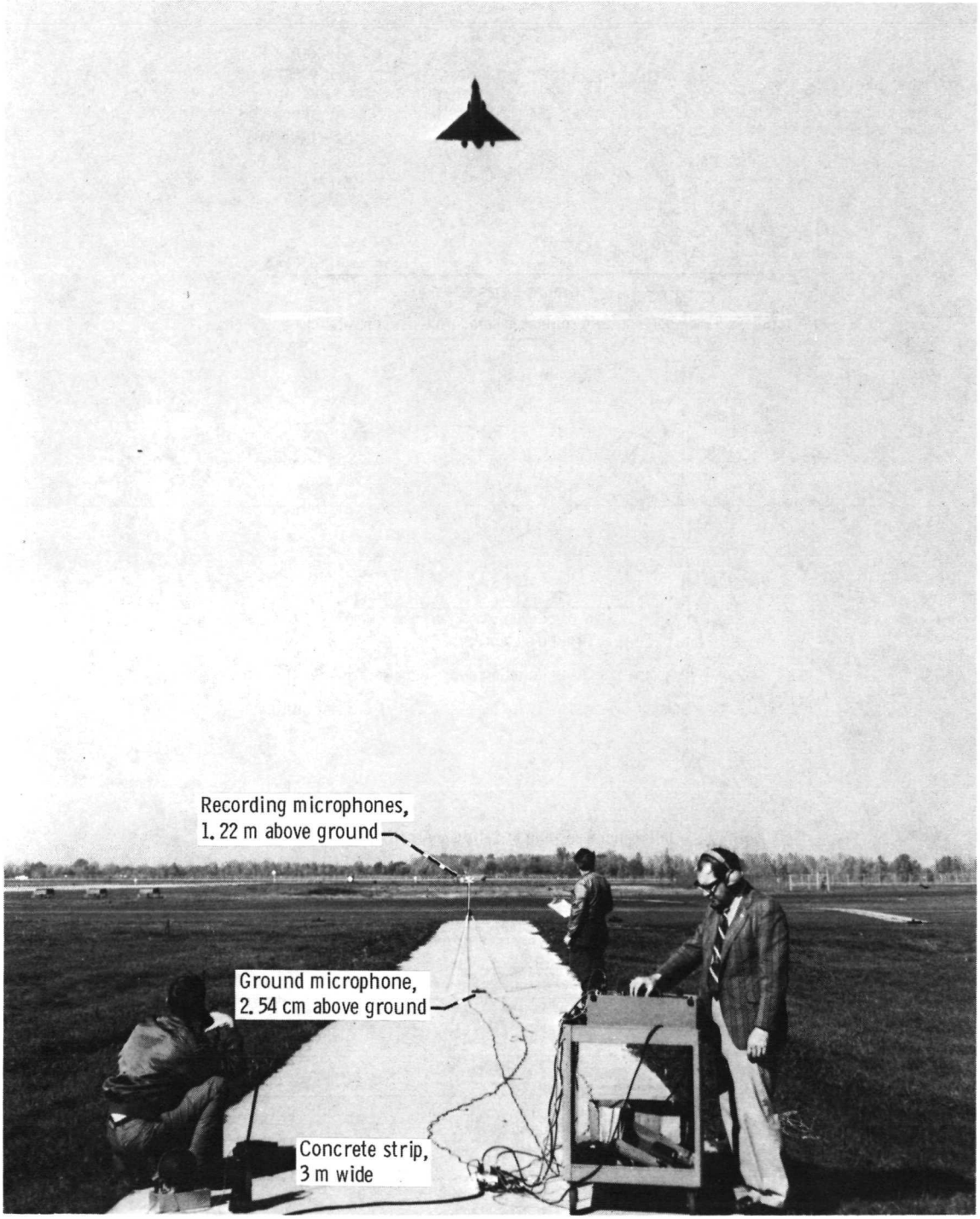

Figure 15. - Sound flyover showing microphone position and recording equipment.

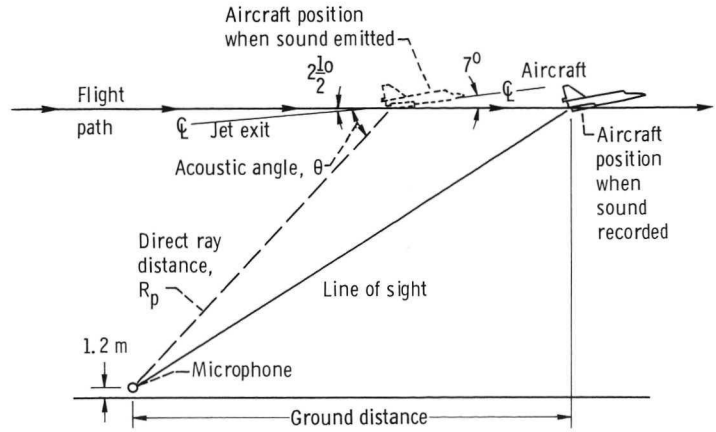

(a) Aircraft position when emitting sound compared with visual position when recorded.

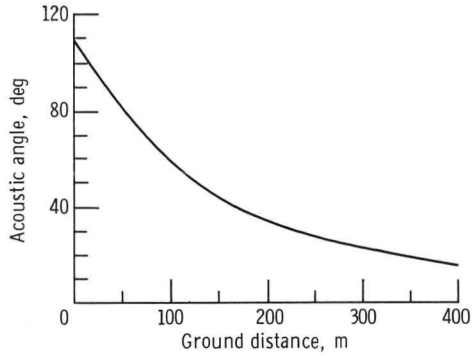

(b) Acoustic angle as function of ground distance.

Figure 16. - Noise flyover geometry for Mach 0.4 and 91.4-meter altitude.

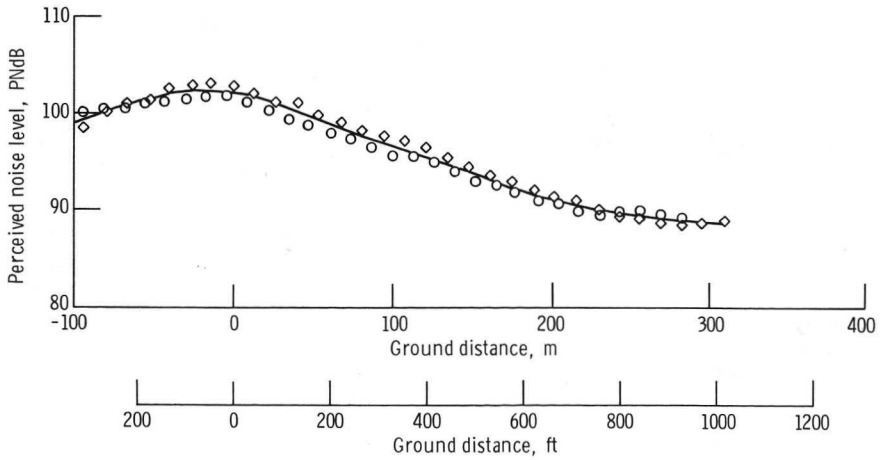

Figure 17. - Flyover background noise level for 91.4-meter altitude and Mach 0.4 adjusted to standard day. Main engine at idle.

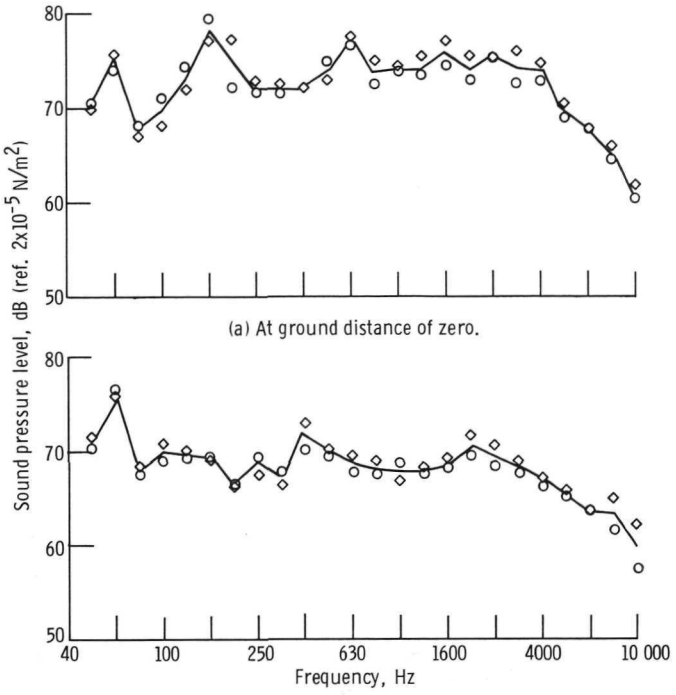

(a) At ground distance of zero.

(b) At ground distance of 100 meters.

Figure 18. - Frequency spectra for background noise during flyover. Adjusted to standard day. One-third-octave bands.

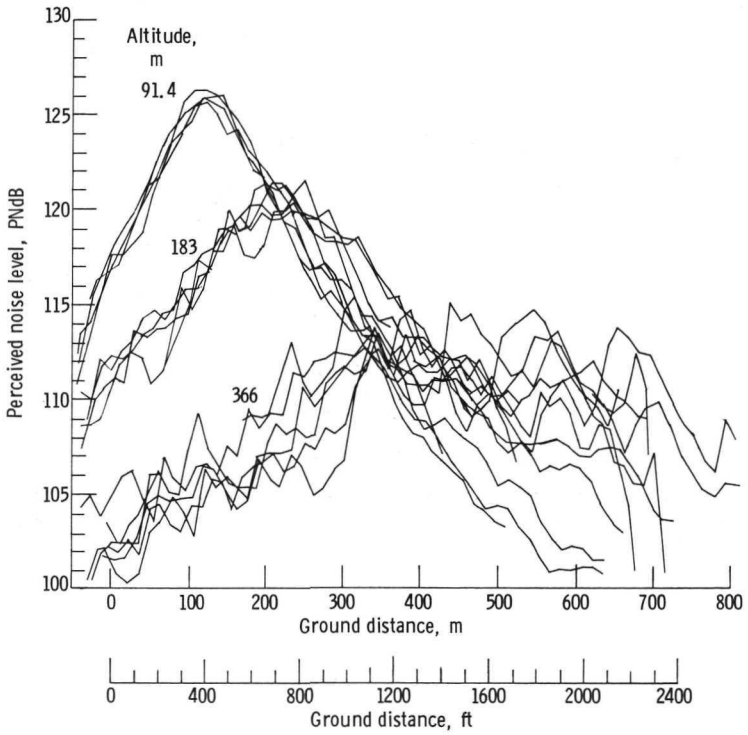

Figure 19. - Repeatability and scatter in flyover noise data for the cylindrical ejector nozzle in maximum afterburner for three altitudes at Mach 0.4.

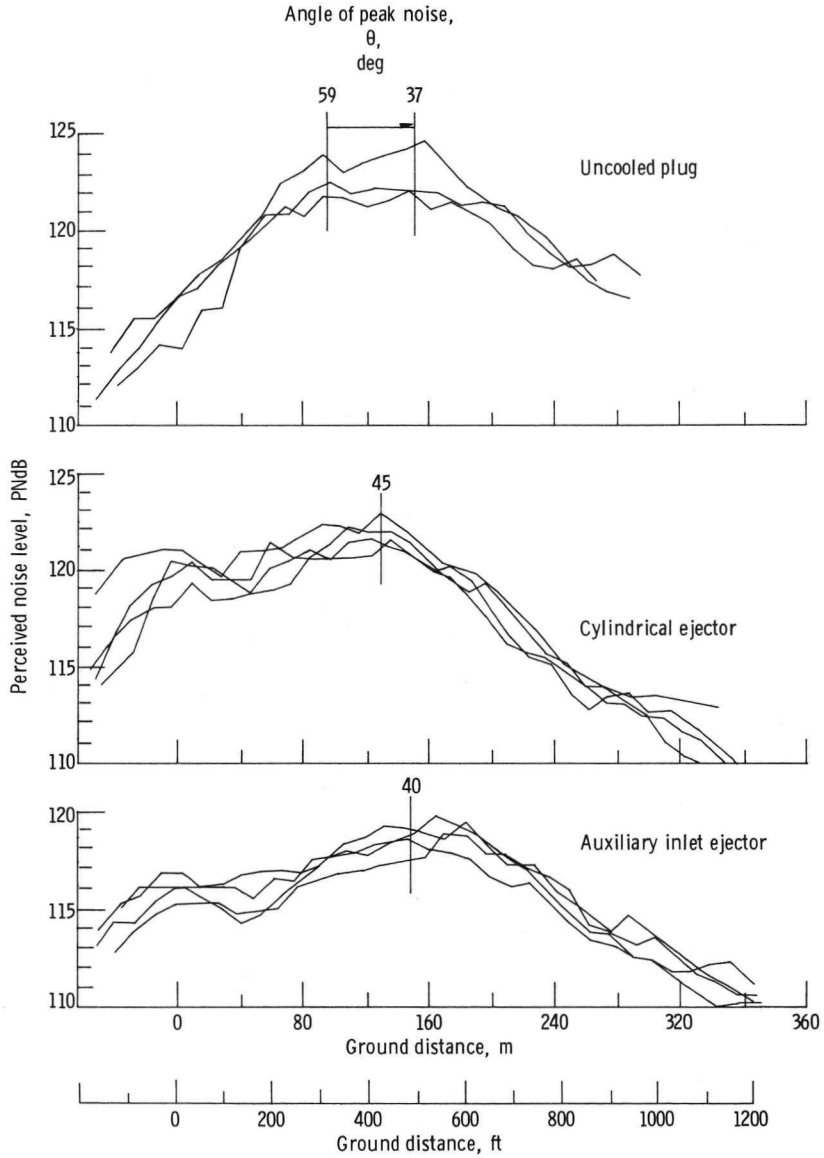

(a) Military power.

Figure 20. - Comparison of three nozzle perceived noise levels as function of distance. Altitude, 91.4 meters; Mach 0.4; adjusted to standard day conditions and relative jet velocity of 560 meters per second.

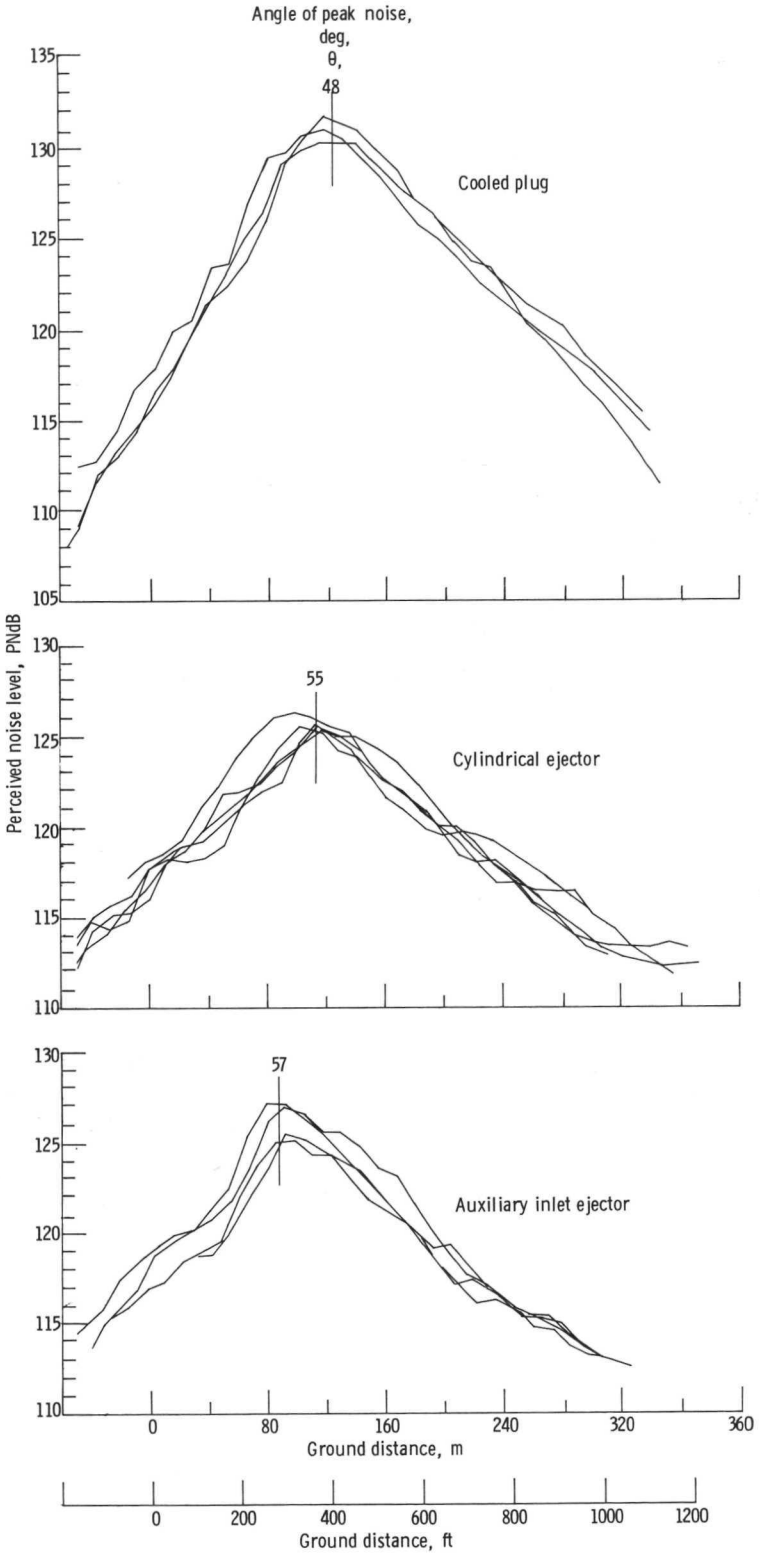

(b) Maximum afterburner power.

Figure 20. - Concluded.

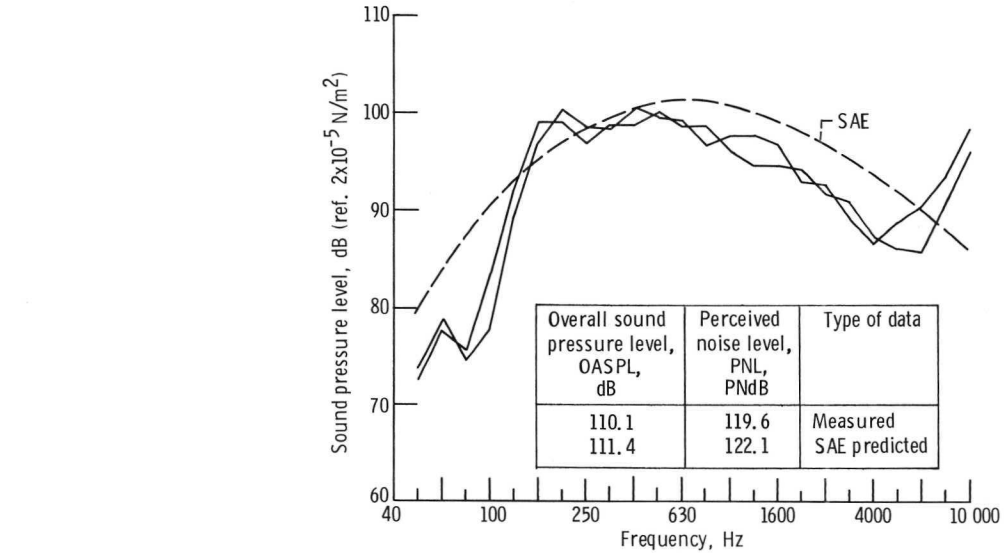

(a) Uncooled plug nozzle.

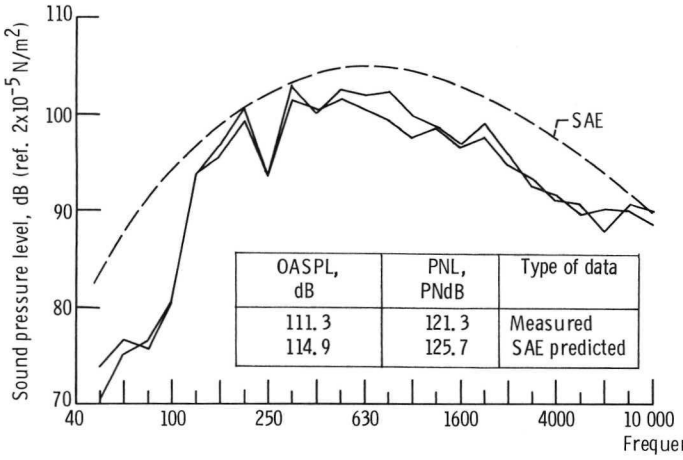

(b) Cylindrical ejector nozzle.

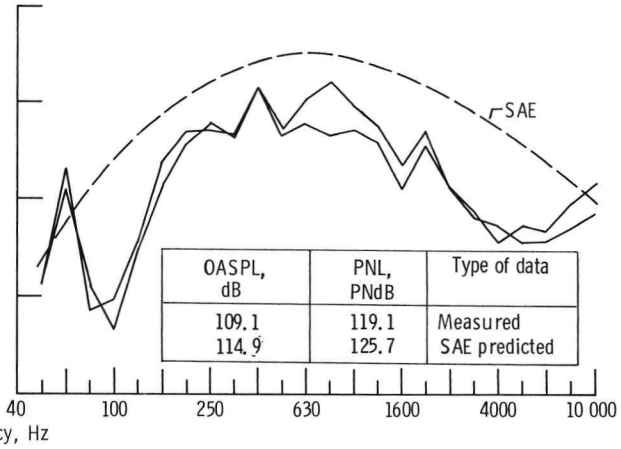

(c) Auxiliary inlet ejector.

Figure 21. - Comparison of measured and SAE predicted spectra at peak noise. Nominal military power; adjusted to standard day. One-third-octave bands.

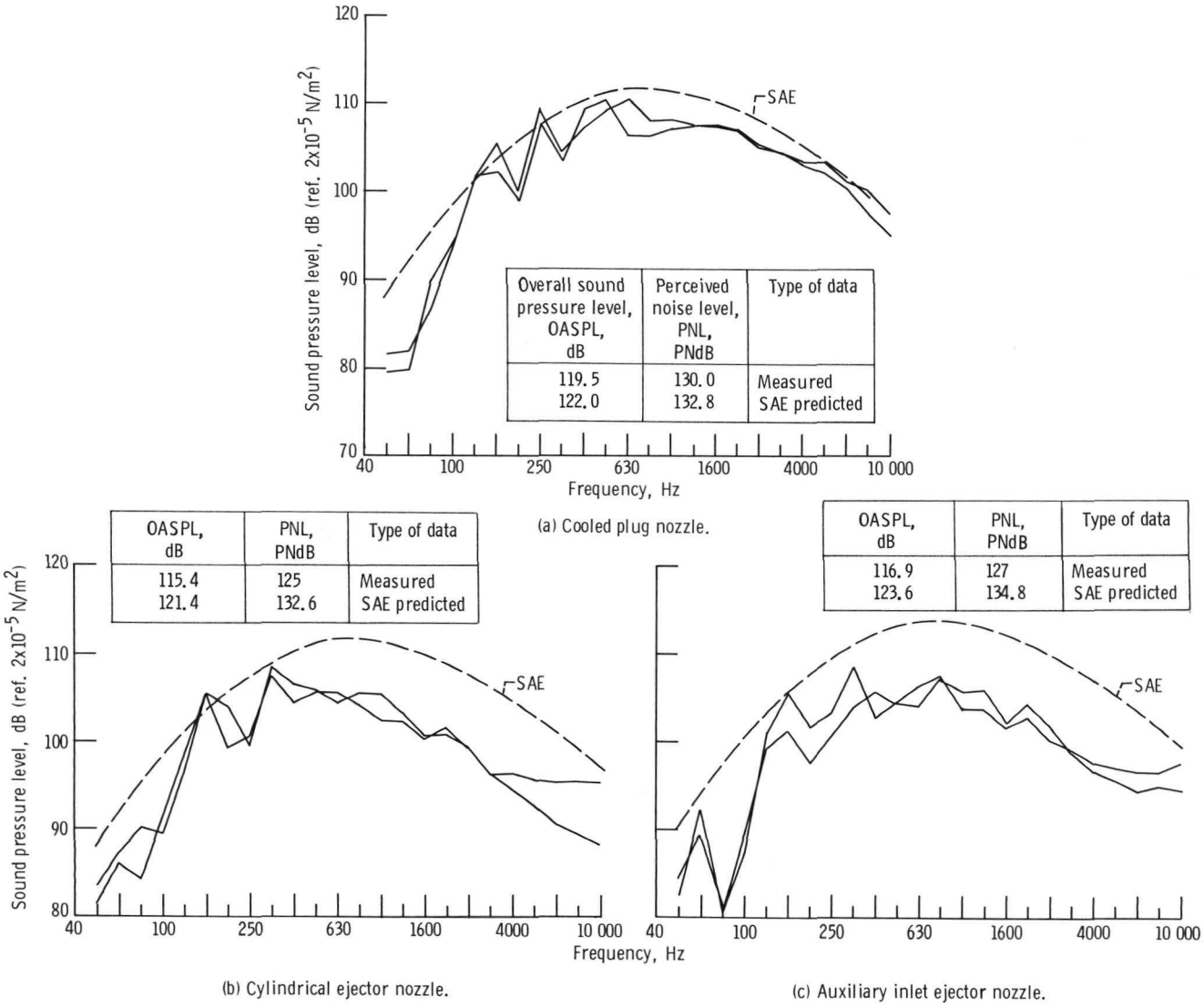

(a) Cooled plug nozzle.

(b) Cylindrical ejector nozzle.

(c) Auxiliary inlet ejector nozzle.

Figure 22. - Comparison of measured and SAE predicted spectra at peak noise. Nominal maximum afterburner power; adjusted to standard day; one-third-octave bands.

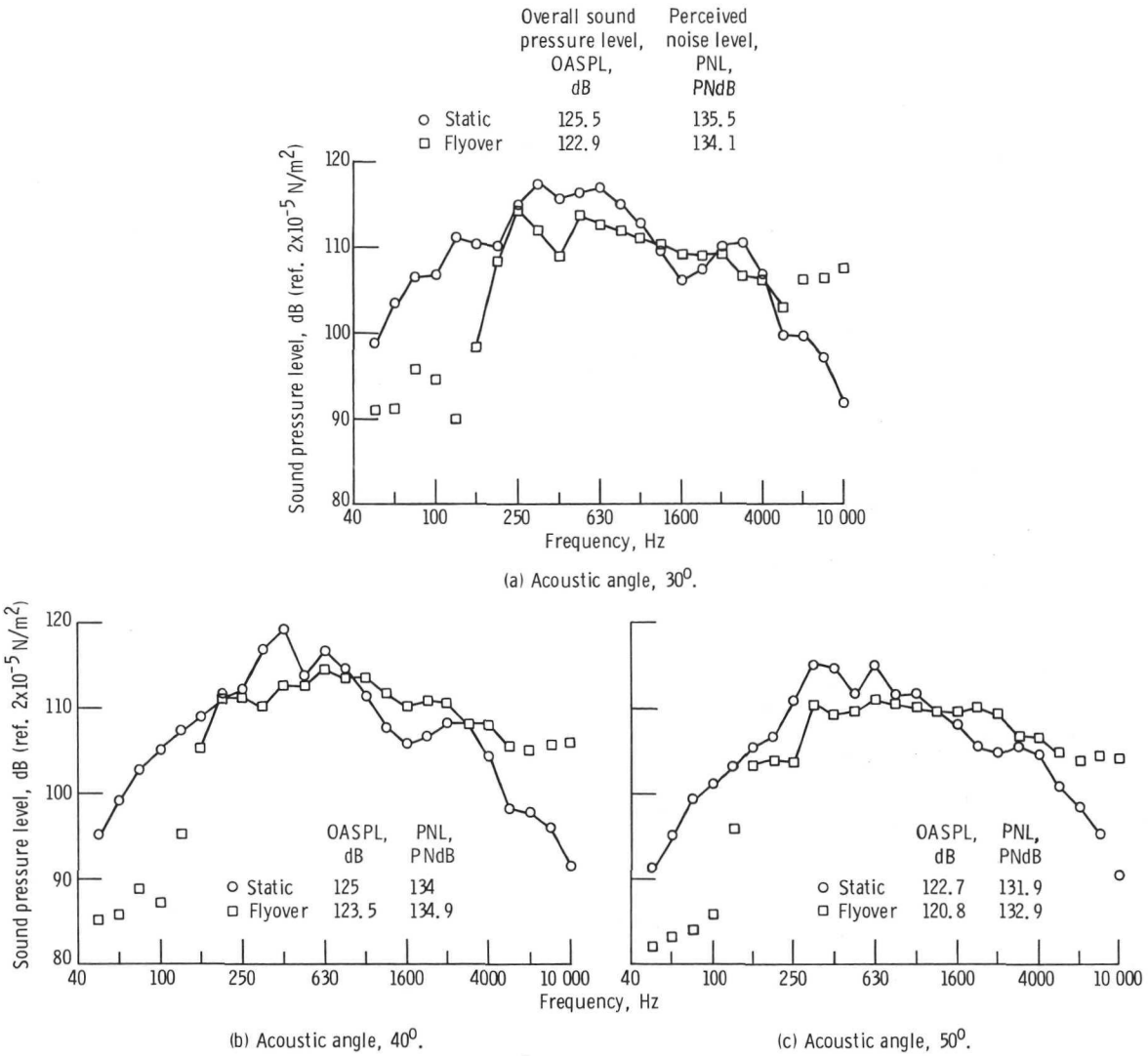

(a) Acoustic angle, 30^{o}.

(b) Acoustic angle, 40^{o}.

(c) Acoustic angle, 50^{o}.

Figure 23. - Comparison of flyover and static spectra for uncooled plug nozzle at 30.48 meters from nozzle. Relative jet velocity, 600 meters per second; one-third-octave bands.

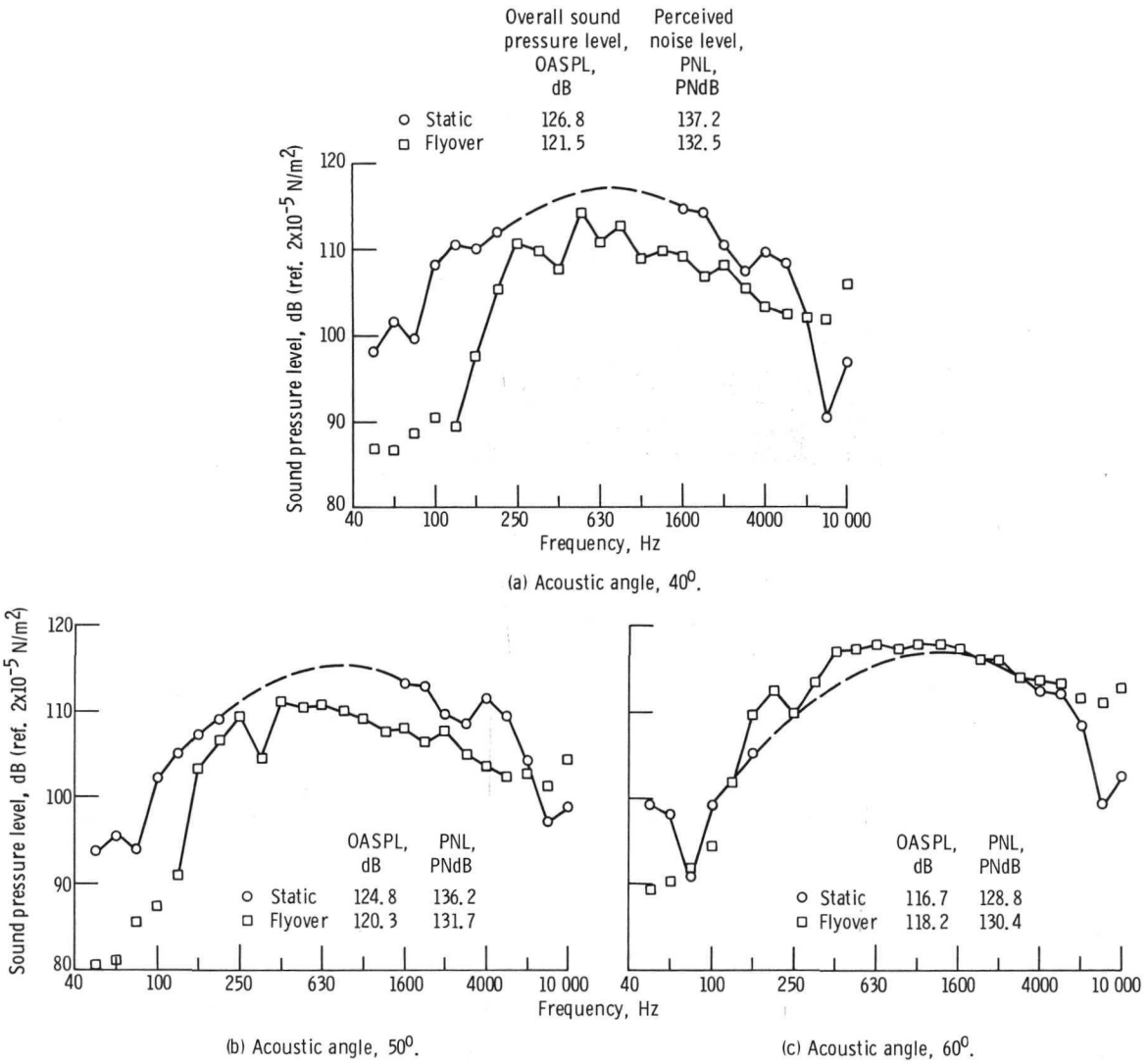

Figure 24. - Comparison of flyover and static spectra for cylindrical ejector nozzle at 30.48 meters from nozzle. Relative jet velocity, 600 meters per second; one-third-octave spectra.

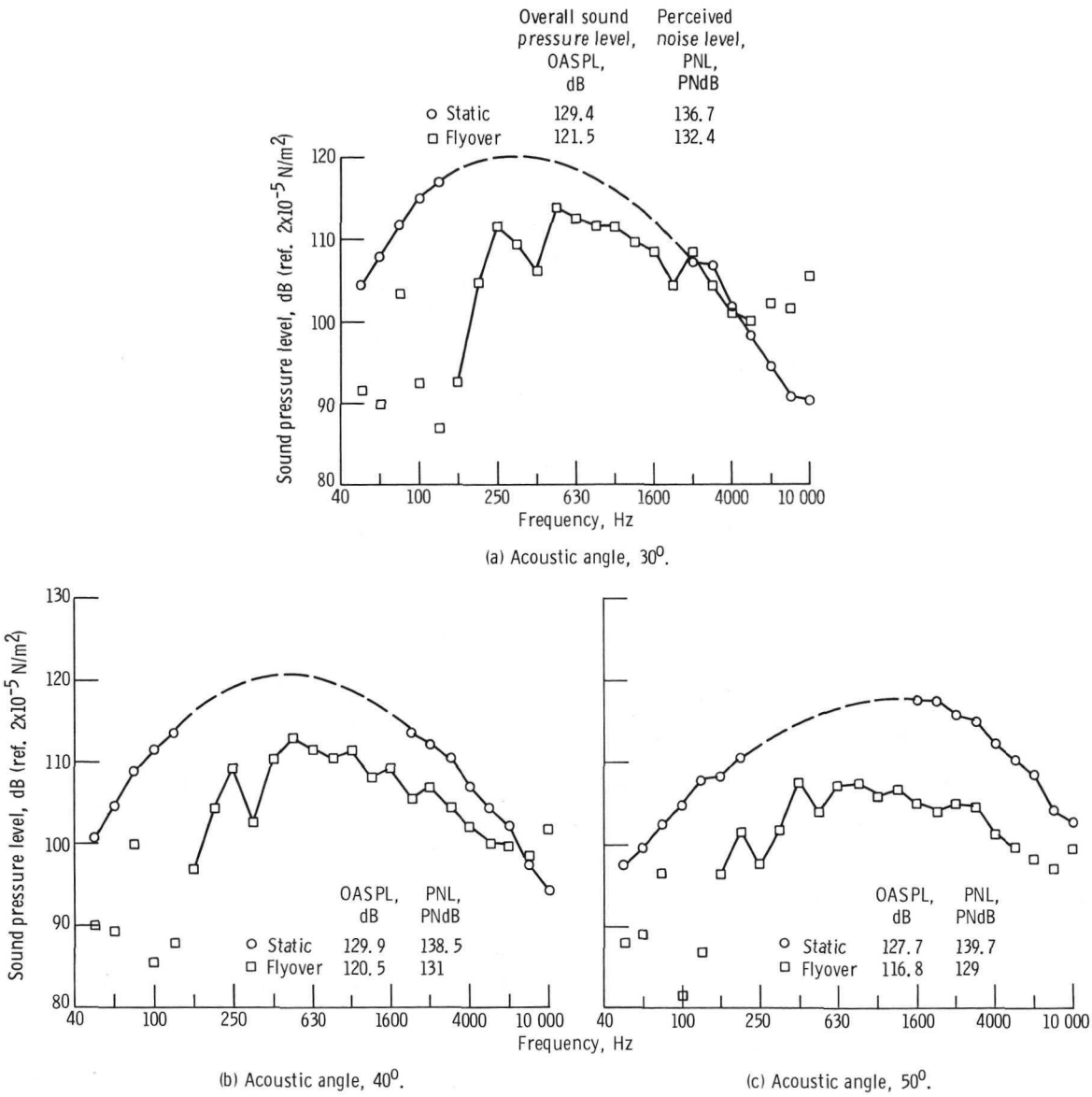

Figure 25. - Comparison of flyover and static spectra for auxiliary inlet ejector nozzle at 30.48 meters from nozzle. Relative jet velocity, 600 meters per second; one-third-octave bands.

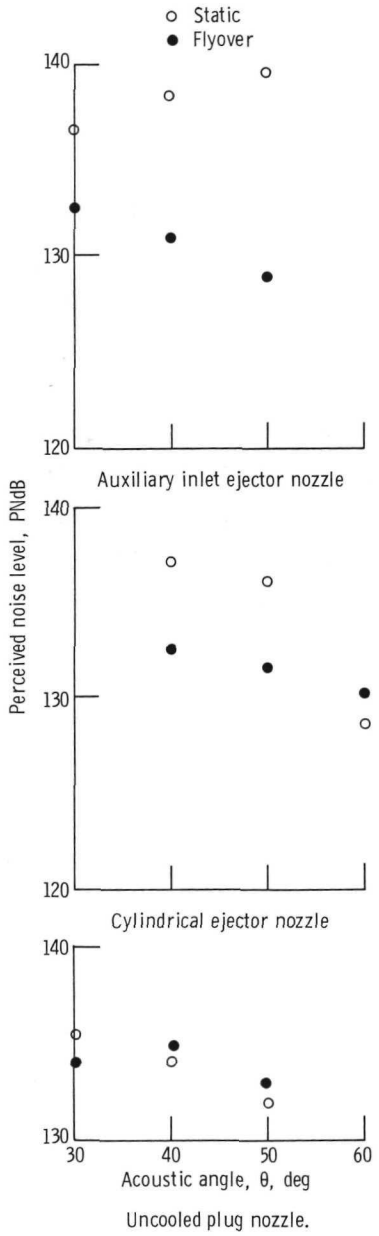

Figure 26. - Comparison of flyover and static noise directivity at 30.48 meters from exhaust nozzle.

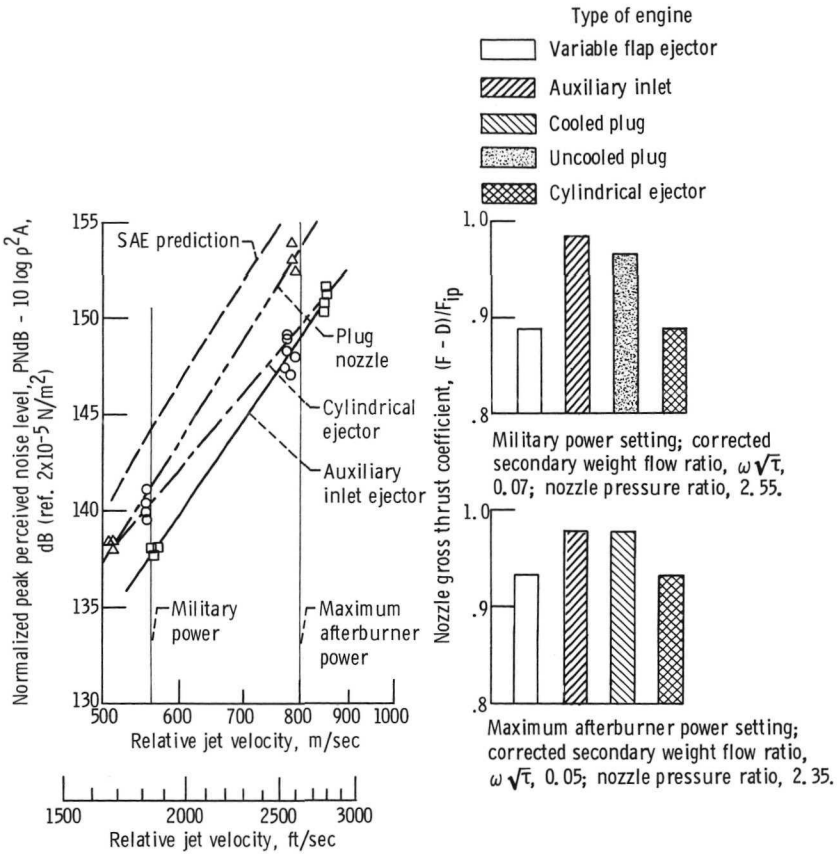

Figure 27. - Comparison of thrust and acoustic characteristics. Flyover at 0.4 Mach number and 91 meter (300 ft) altitude.

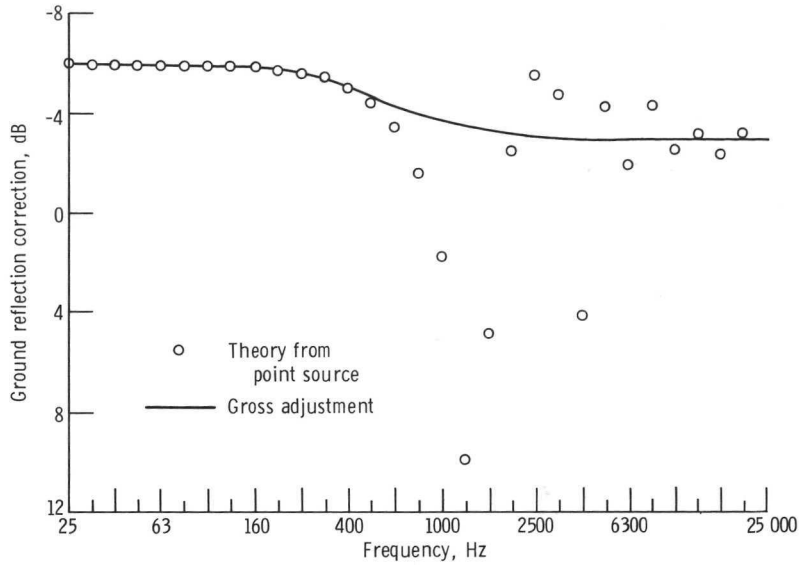

(a) Adjustment from concrete to free field.

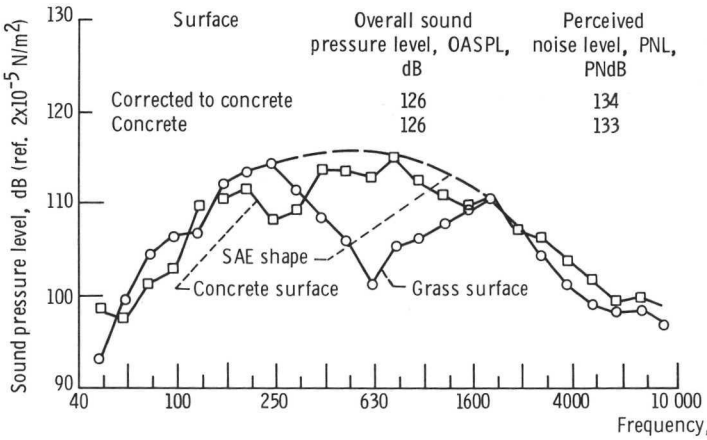

(b) Adjustment from grass to concrete surface; cylindrical ejector nozzle.

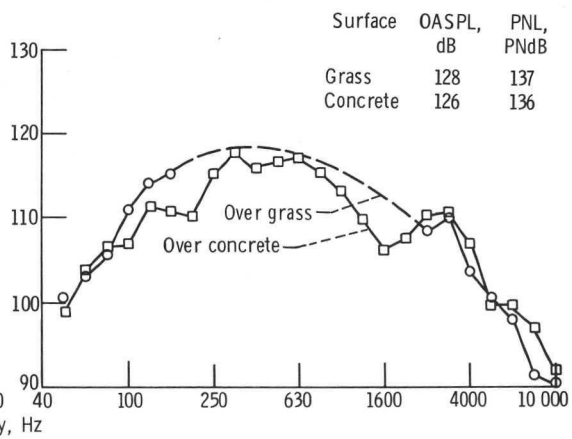

(c) Comparison of adjusted static spectra taken over grass and concrete. Plug nozzle; acoustic angle, 30^0.

Figure 28. - Adjustments to measured static one-third-octave spectra.

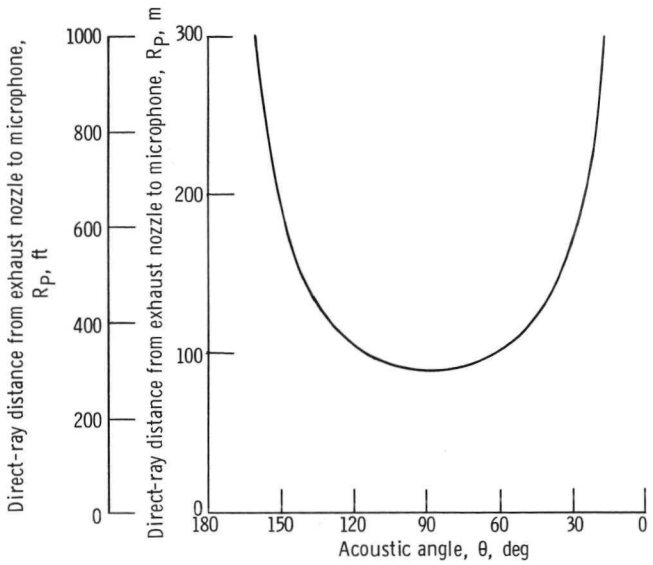

(a) Geometry.

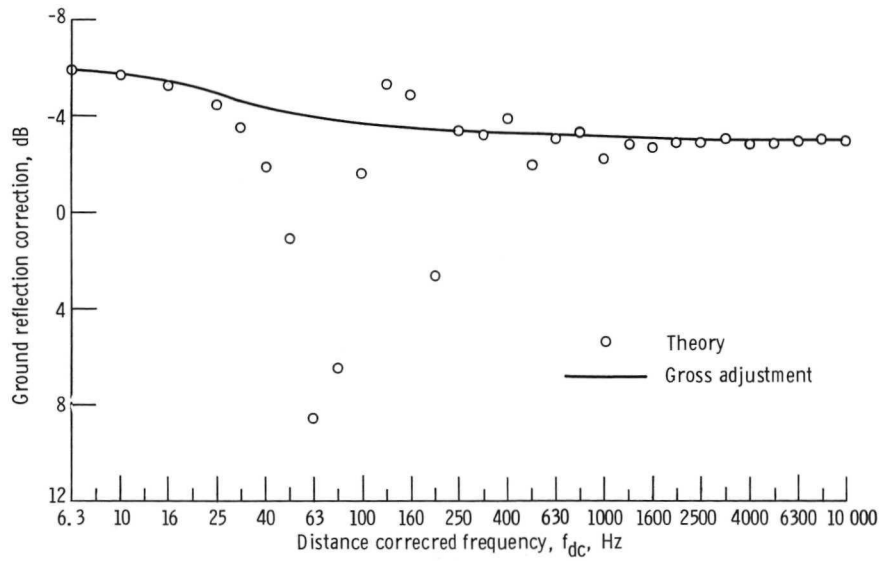

(b) Adjustment from concrete to free-field.

Figure 29. - Flyover geometry and adjustments to spectra.

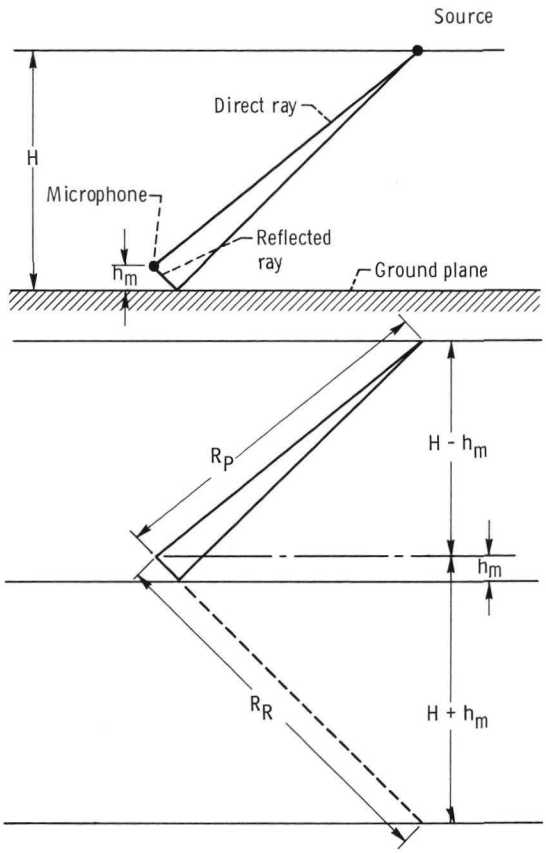

(c) Ground reflection geometry.

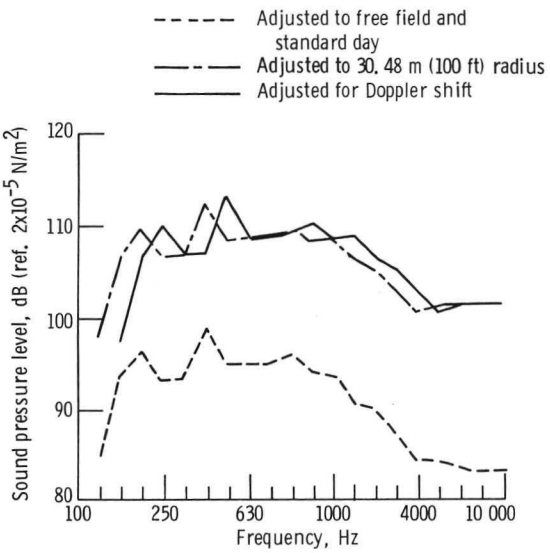

(d) Adjustments to spectra.

Figure 29 - Concluded.

NATIONAL AERONAUTICS AND SPACE ADMINISTRATION
WASHINGTON, D.C. 20546

OFFICIAL BUSINESS
PENALTY FOR PRIVATE USE $300

SPECIAL FOURTH-CLASS RATE
BOOK

POSTAGE AND FEES PAID
NATIONAL AERONAUTICS AND
SPACE ADMINISTRATION
451

U.S.MAIL

POSTMASTER: If Undeliverable (Section 158 Postal Manual) Do Not Return

"The aeronautical and space activities of the United States shall be conducted so as to contribute . . . to the expansion of human knowledge of phenomena in the atmosphere and space. The Administration shall provide for the widest practicable and appropriate dissemination of information concerning its activities and the results thereof."

—NATIONAL AERONAUTICS AND SPACE ACT OF 1958

NASA SCIENTIFIC AND TECHNICAL PUBLICATIONS

TECHNICAL REPORTS: Scientific and technical information considered important, complete, and a lasting contribution to existing knowledge.

TECHNICAL NOTES: Information less broad in scope but nevertheless of importance as a contribution to existing knowledge.

TECHNICAL MEMORANDUMS: Information receiving limited distribution because of preliminary data, security classification, or other reasons. Also includes conference proceedings with either limited or unlimited distribution.

CONTRACTOR REPORTS: Scientific and technical information generated under a NASA contract or grant and considered an important contribution to existing knowledge.

TECHNICAL TRANSLATIONS: Information published in a foreign language considered to merit NASA distribution in English.

SPECIAL PUBLICATIONS: Information derived from or of value to NASA activities. Publications include final reports of major projects, monographs, data compilations, handbooks, sourcebooks, and special bibliographies.

TECHNOLOGY UTILIZATION PUBLICATIONS: Information on technology used by NASA that may be of particular interest in commercial and other non-aerospace applications. Publications include Tech Briefs, Technology Utilization Reports and Technology Surveys.

Details on the availability of these publications may be obtained from:

SCIENTIFIC AND TECHNICAL INFORMATION OFFICE

NATIONAL AERONAUTICS AND SPACE ADMINISTRATION

Washington, D.C. 20546